Higgs boson production and decay rate measurements and their interpretation with the ATLAS experiment

Weitao Wang
on behalf of the ATLAS collaboration

Lake Louise Winter Institute 2024
19.02.2024

Since Higgs Boson discovery

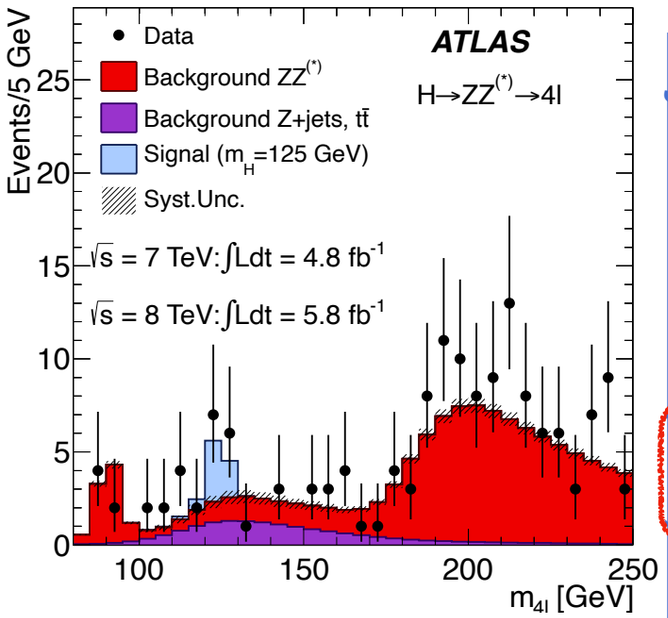

Phys. Lett. B 716 (2012) 1-29

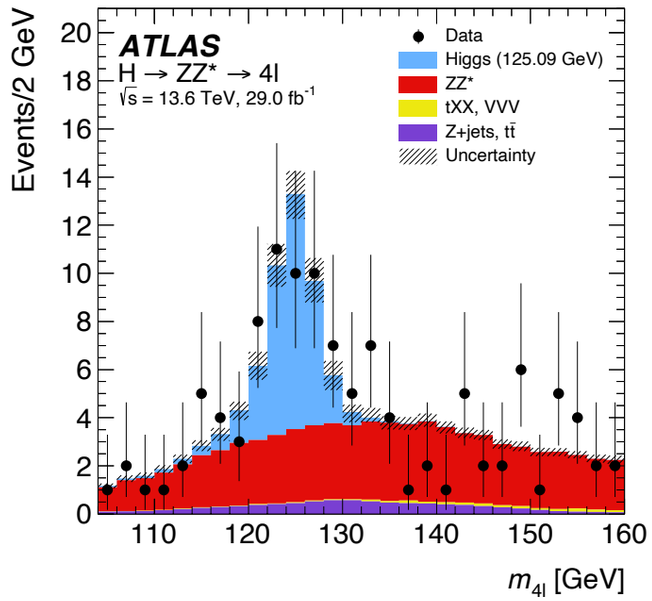

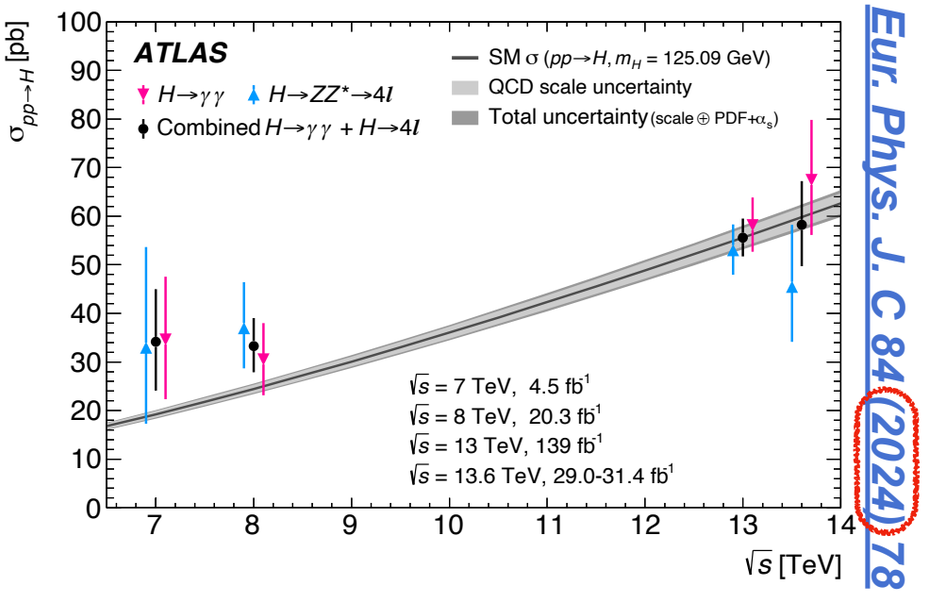

Eur. Phys. J. C 84 (2024) 78

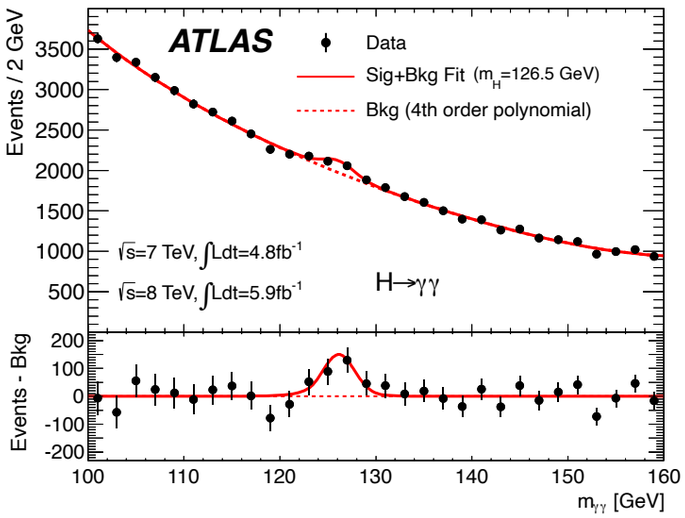

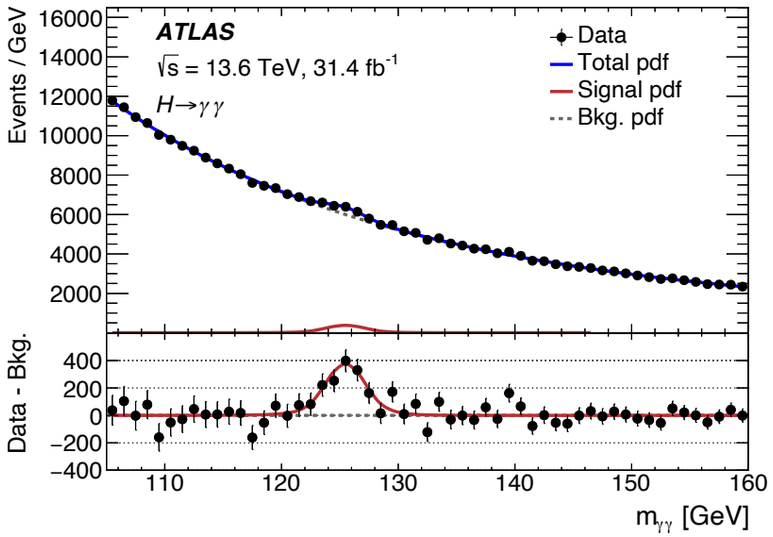

- ATLAS Run 3, 2022 data
- First measurement at $\sqrt{s} = 13.6$ TeV

Higgs boson has been found for more than 10 years, yet there are still a lot of unanswered questions

- Precision measurements of Higgs boson properties
- Search for Higgs decays into 2nd generation fermions, and rare decays
- Higgs measurement in high p_T kinematic regions

The Higgs boson plays a key role in exploring the physics beyond the SM

Higgs production and decay modes

Production

gluon-gluon fusion (ggF)

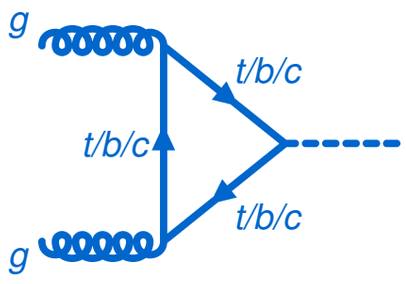

Vector-boson-fusion (VBF)

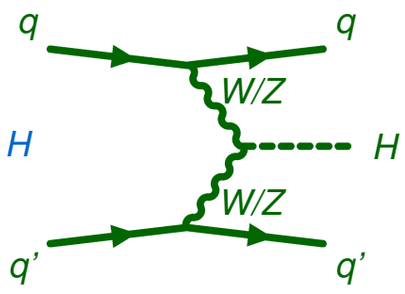

Associated production with a vector boson (VH)

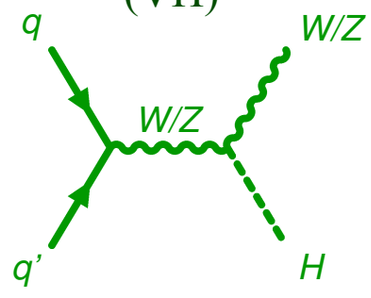

Associated production with a top or bottom pair (ttH/bbH)

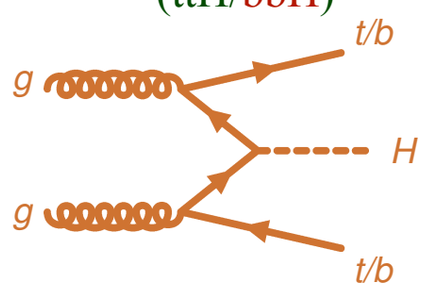

Associated production with a single top (tH)

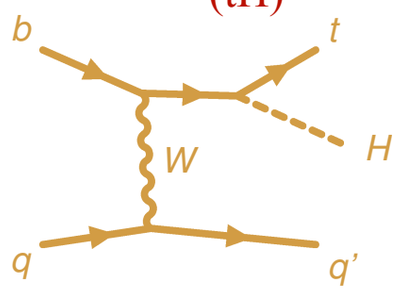

Observed ($> 5\sigma$)
Not observed yet ($< 5\sigma$)

Decay

$H \to WW, H \to ZZ$

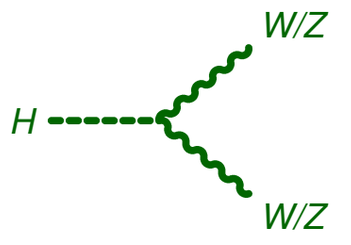

$H \to \gamma\gamma$, $H \to Z\gamma$

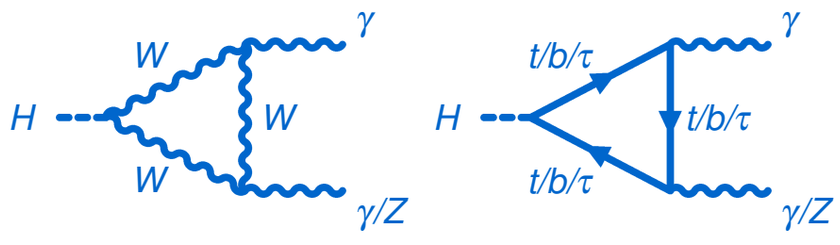

$H \to b\bar{b}$, $H \to c\bar{c}$

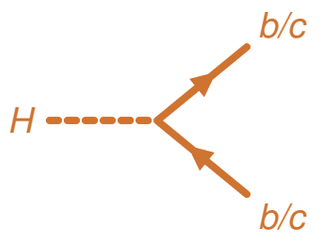

$H \to \tau^+\tau^-$, $H \to \mu^+\mu^-$

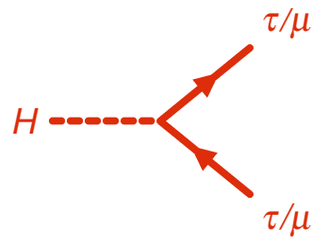

An overview of ATLAS Run 2 results

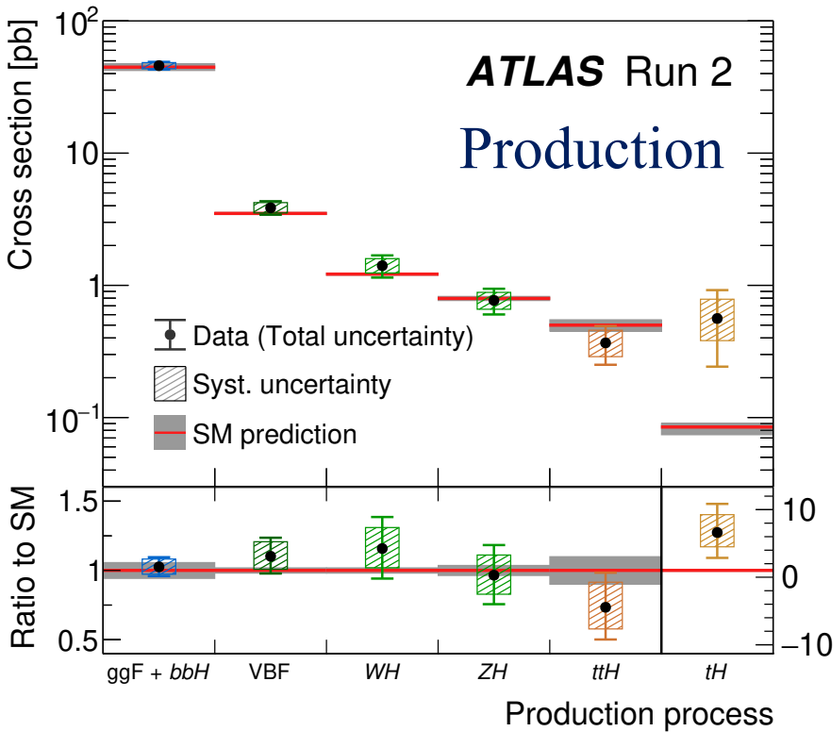

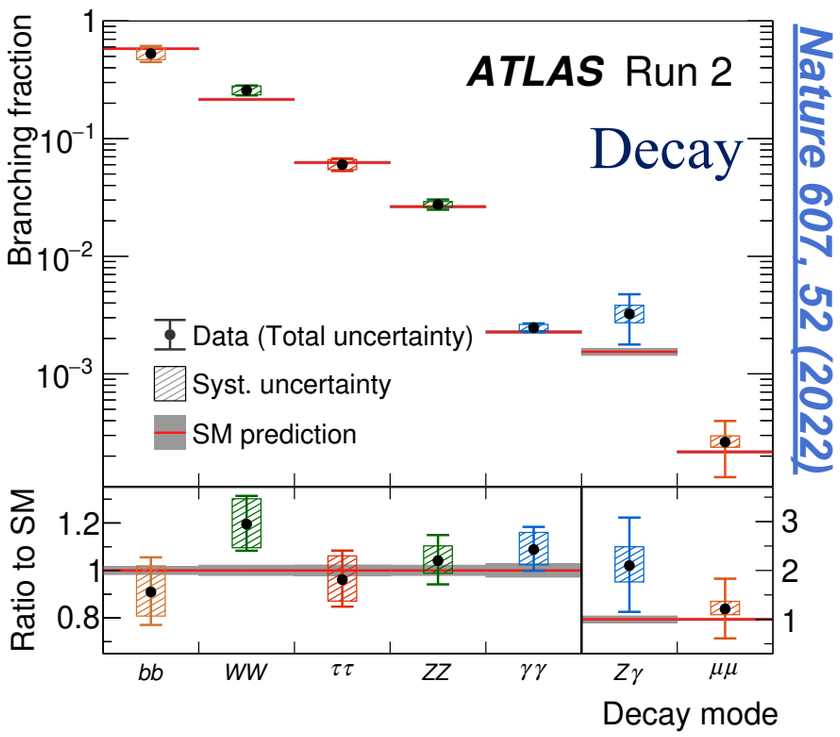

Nature 607, 52 (2022)

Cross-section and κ-framework

- Provided multiple measurements of the various production modes in the different decays channels
- We can interpret in a coherent way to probe for possible BSM effects

κ-framework

- Use a set of coupling strength modifiers κ to express modification with respect to SM predictions and probe possible BSM effects

$$\sigma(i \to H \to f) = \sigma_i \cdot B_f = \frac{\sigma_i^{SM} \cdot \Gamma_f^{SM}}{\Gamma_H^{SM}} \cdot \frac{\kappa_i^2 \cdot \kappa_f^2}{\kappa_H^2}, \text{ where } \kappa_i^2 = \frac{\sigma_i}{\sigma_i^{SM}}, \quad \kappa_f^2 = \frac{\Gamma_f}{\Gamma_f^{SM}} \qquad SM \to \kappa = 1$$

- κ_H is related to the total width of Higgs boson, including self-coupling and invisible decays

Only SM effect allow ***non-SM effect allowed***

Nature 607, 52 (2022)

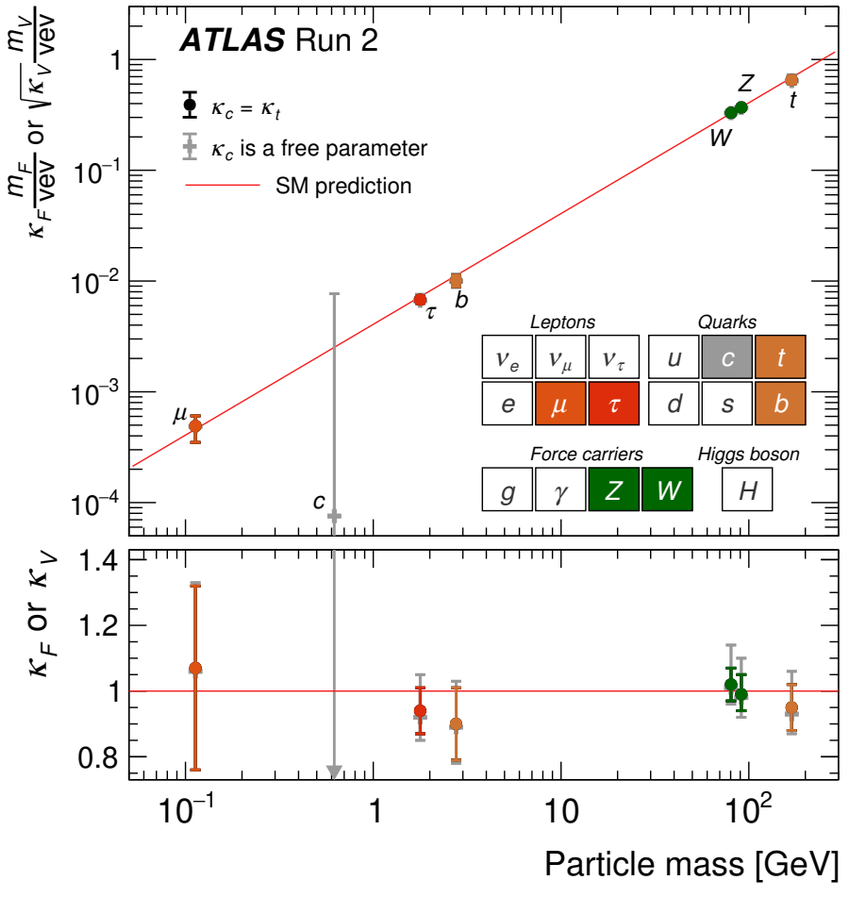

Compatibility to SM

56% ($\kappa_c = \kappa_t$)

65% (κ_c free)

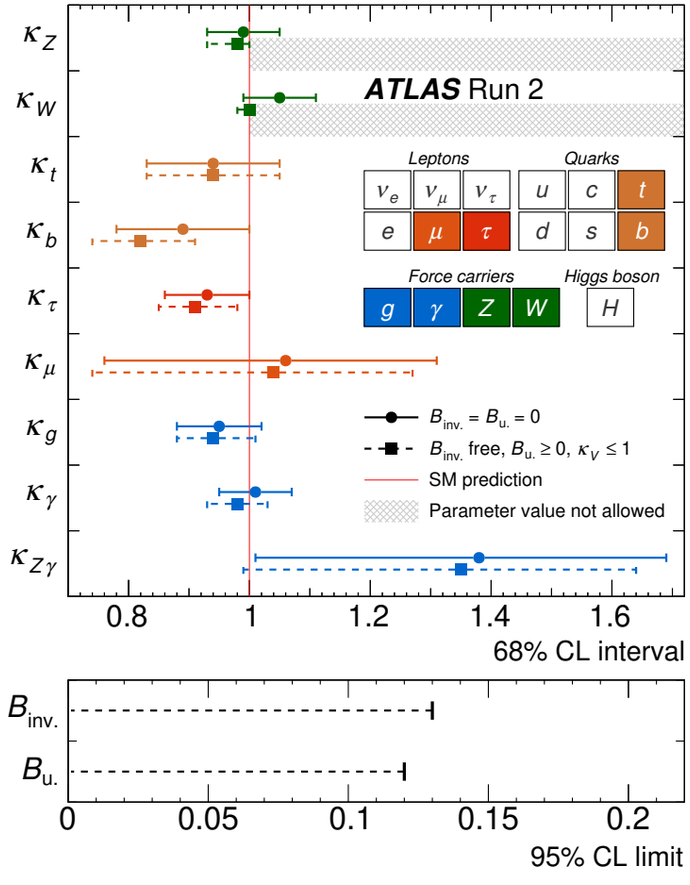

Compatibility to SM

61% ($B_{inv.} = B_u = 0$)

Beyond total cross-section measurement

Fiducial and differential cross section measurements

- Done in specific phase space regions
- Measure cross section in bins of some observables
- The shape information provided by differential cross sections can be exploited for a range of further interpretations

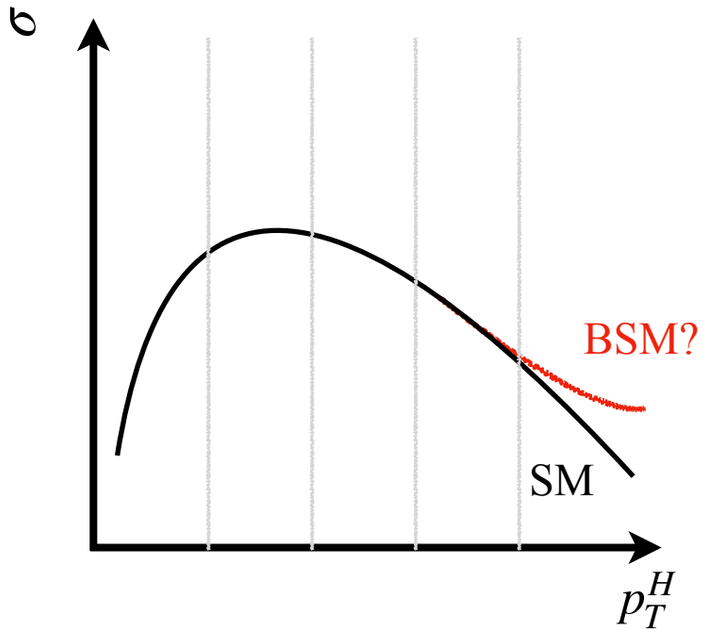

Simplified template cross-section (STXS)

- Done for each production mode
- Define regions by the specific kinematic properties of the Higgs boson and associated jets, W or Z
- Design a simple template but sensitivity to deviations from the SM predictions

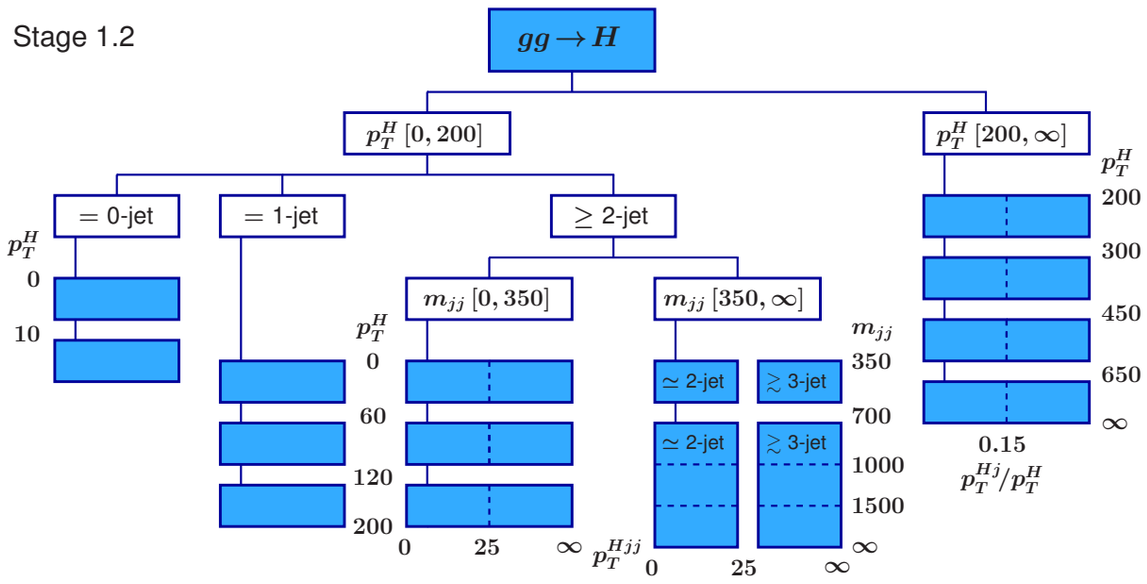

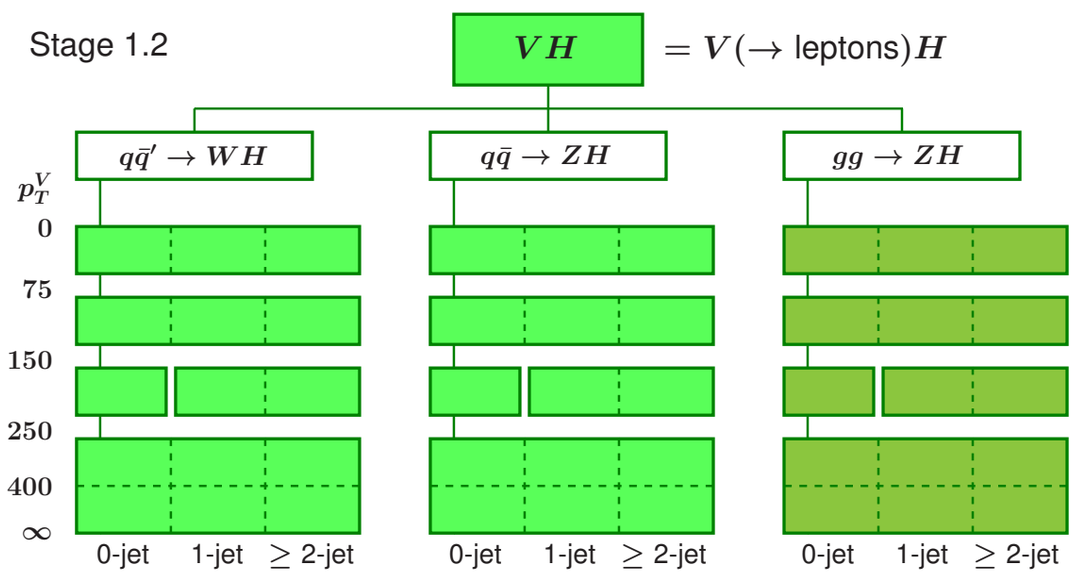

Search for beyond SM effect — EFT interpretation

Standard Model Effective Field Theory (EFT)

$$\mathscr{L}_{SMEFT} = \mathscr{L}_{SM} + \sum_{i}^{N_{d=6}} \frac{c_i}{\Lambda^2} \mathcal{O}_i^{(6)} + \sum_{j}^{N_{d=8}} \frac{b_j}{\Lambda^4} \mathcal{O}_j^{(8)} + \ldots,$$

- $\mathcal{O}_i$ represent a complete set of operators of mass-dimensions
- c_i, b_j are the corresponding dimensionless Wilson coefficients

- Can reflect the effect from a wide class of BSM theories
- Provide a common language to describe the BSM effect in all Higgs analysis

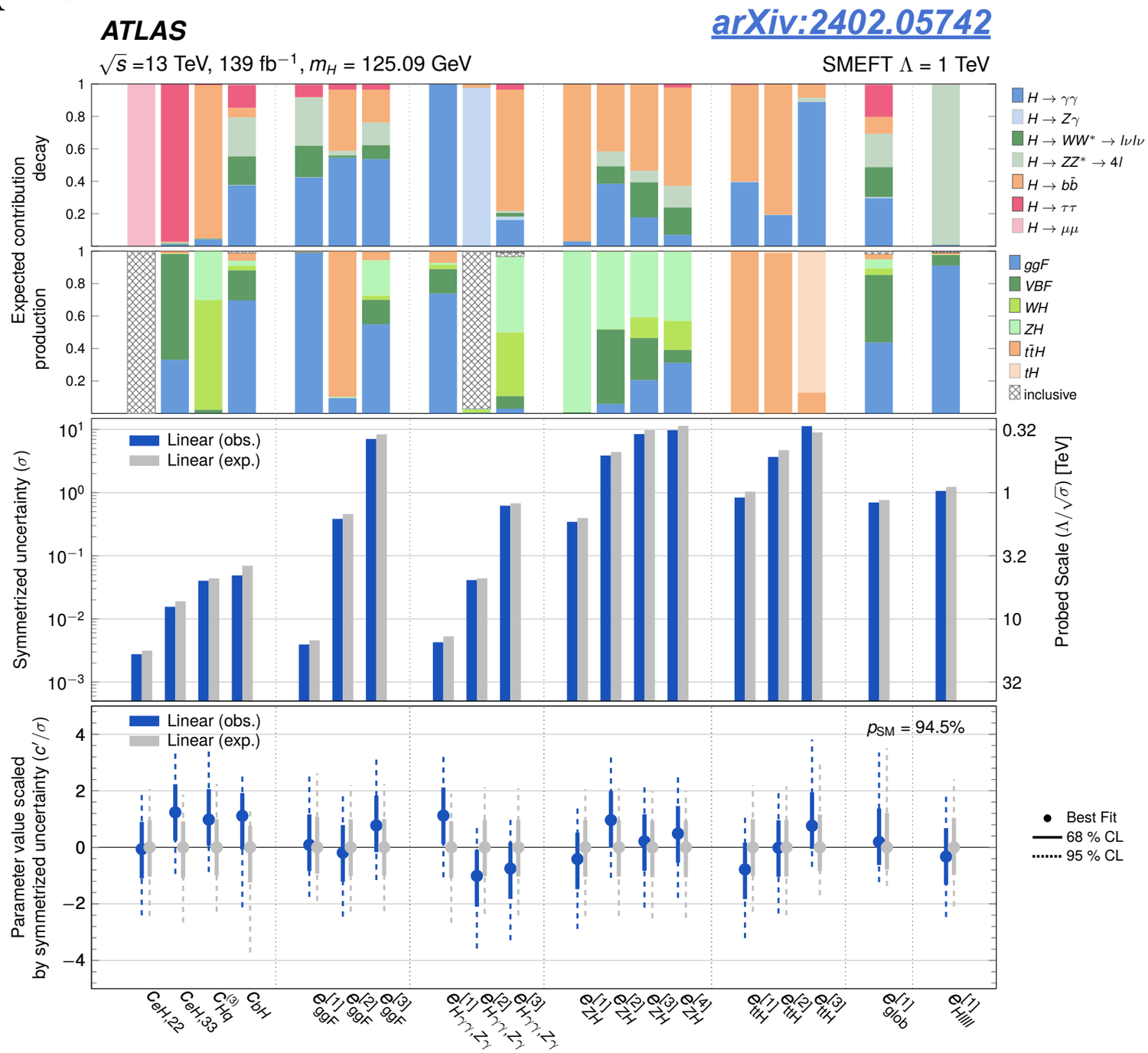

$H \to ZZ^* \to 4\ell$ and $H \to \gamma\gamma$

Differential cross-section measurements

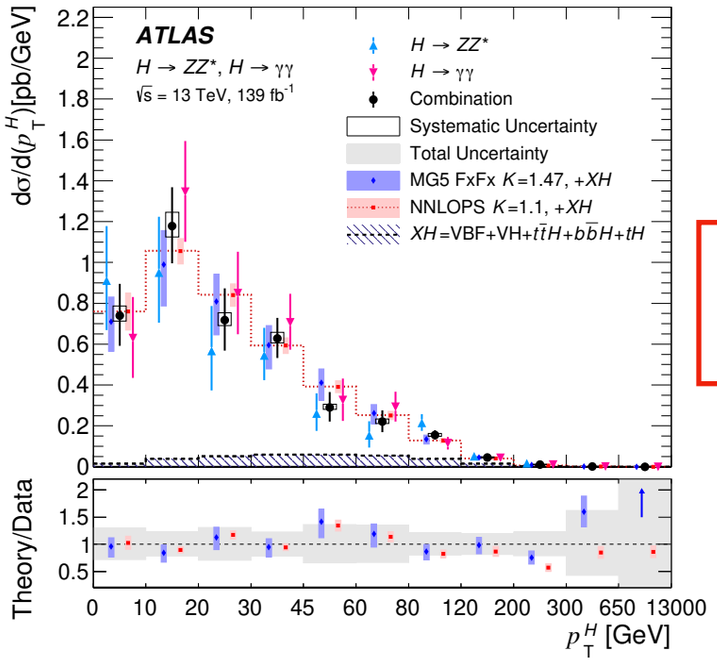

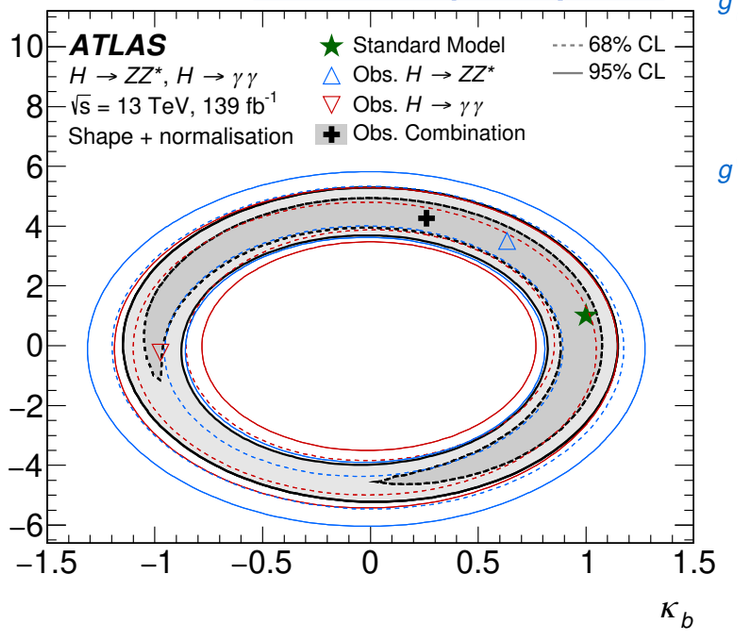

[JHEP 05 (2023) 028](#)

Indirect constraints of Yukawa couplings

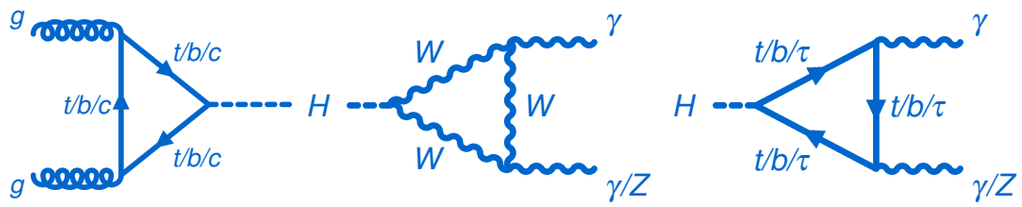

- The loops contain the information of the Yukawa couplings
- The p_T^H shape can be used to constrain κ_b, κ_c

EFT interpretations from STXS measurements

ZZ [Eur. Phys. J. C 80 (2020) 957](#)

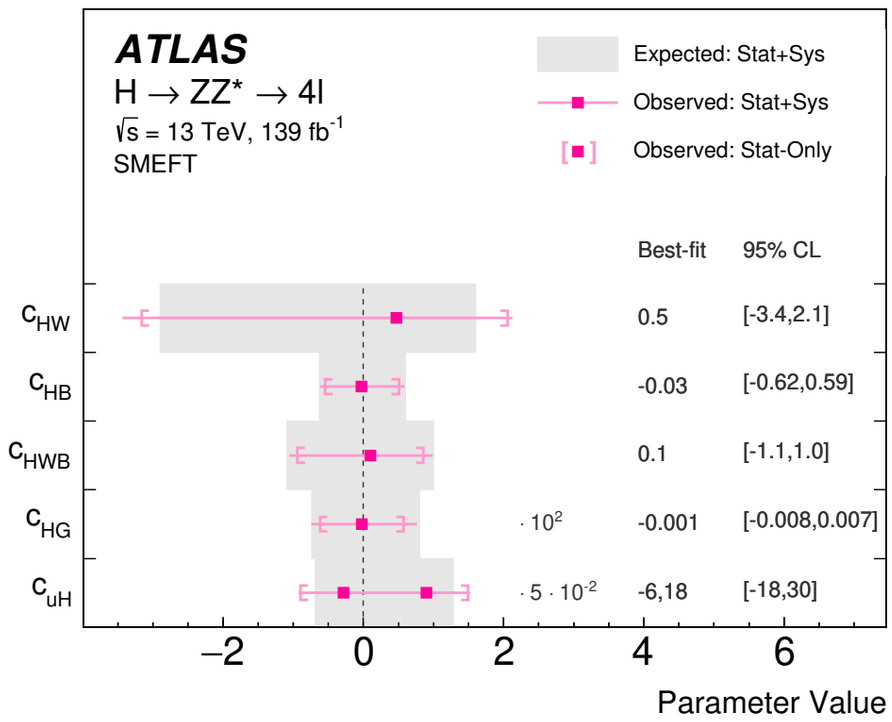

γγ [JHEP 07 (2023) 088](#)

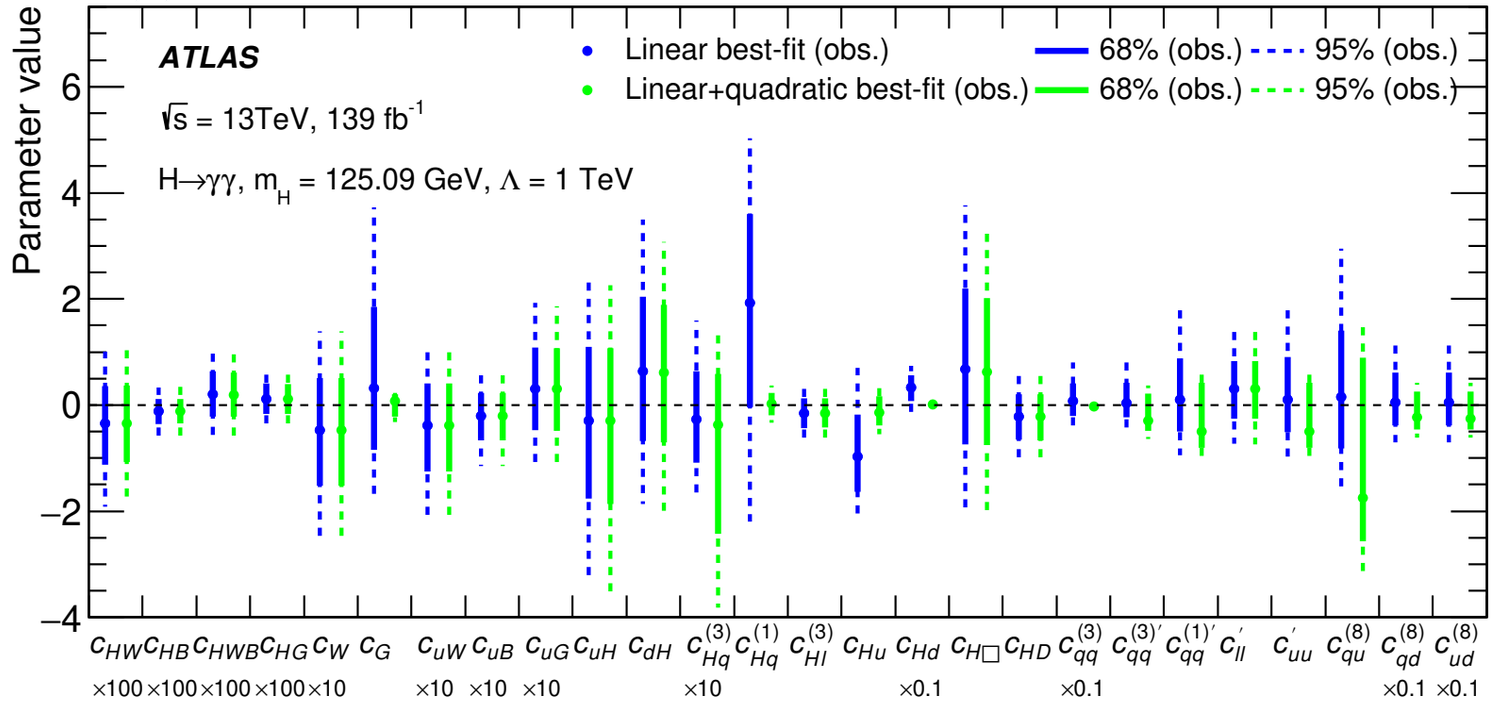

$H \to WW^*$

ggF and VBF production, $e\nu\mu\nu$ final states

- ggF probes couplings to heavy quarks
- VBF probes couplings to W and Z

$$\sigma_{ggF} \cdot \mathcal{B}_{H\to WW^*} = 12.0 \pm 1.4\ pb$$
$$\sigma_{VBF} \cdot \mathcal{B}_{H\to WW^*} = 0.75^{+0.19}_{-0.16}\ pb$$

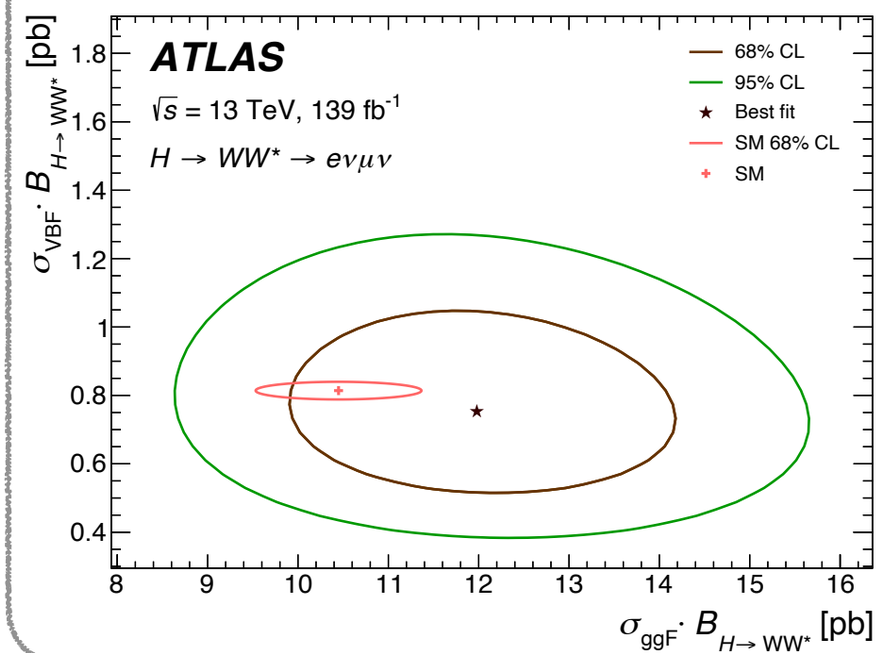

Phys. Rev. D 108 (2023) 032005

VBF differential XS and EFT

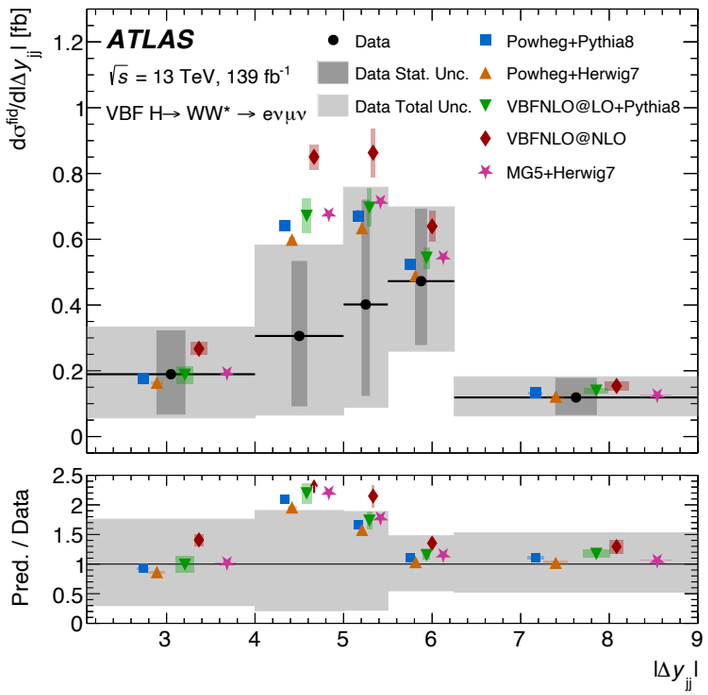

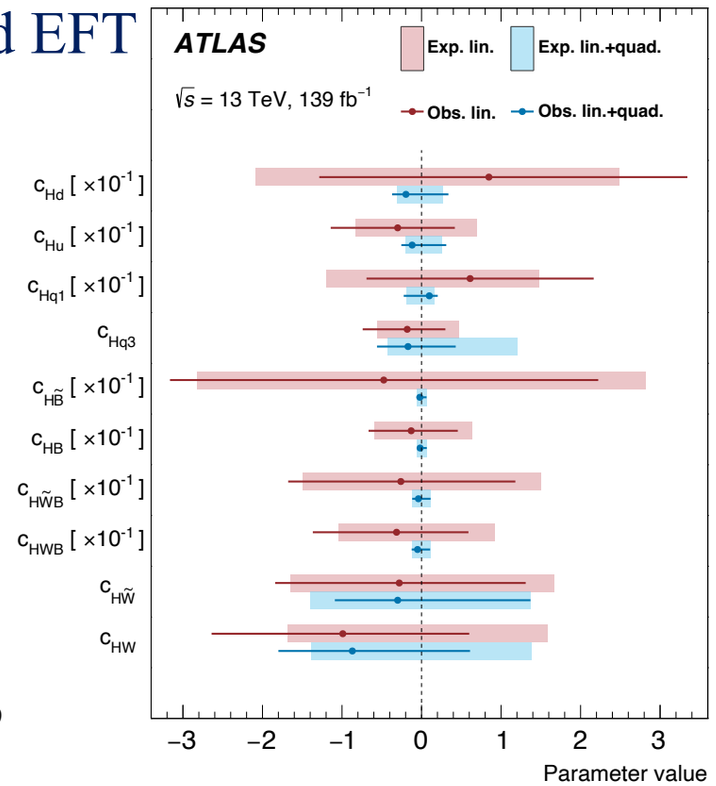

Phys. Rev. D 108 (2023) 072003

ggF differential cross-section

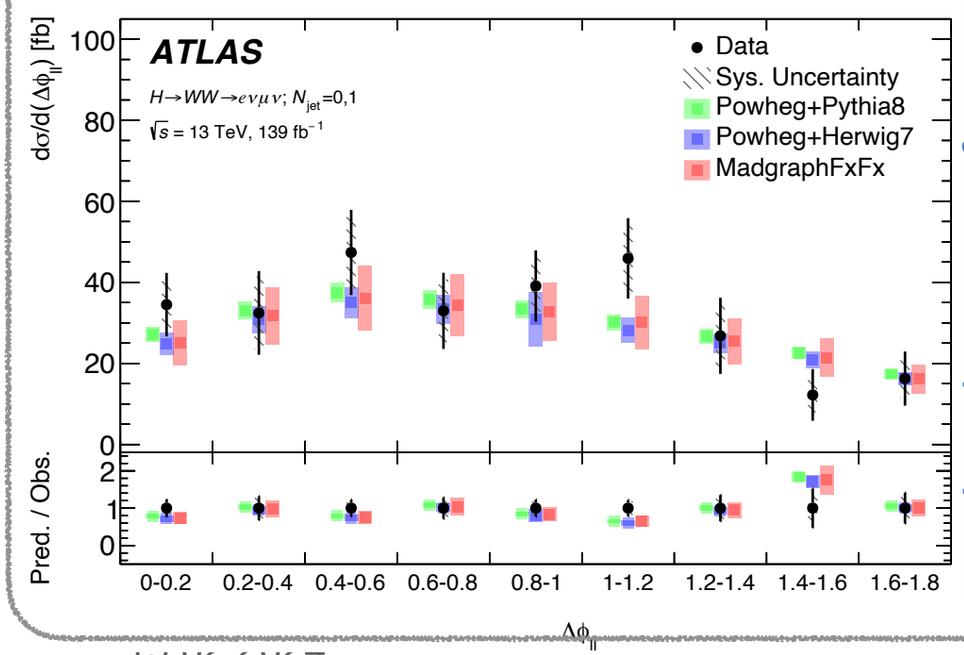

Eur. Phys. J. C 83 (2023) 774

VH production, $\ell\nu\ell\nu$ & $\ell\nu jj$ final states

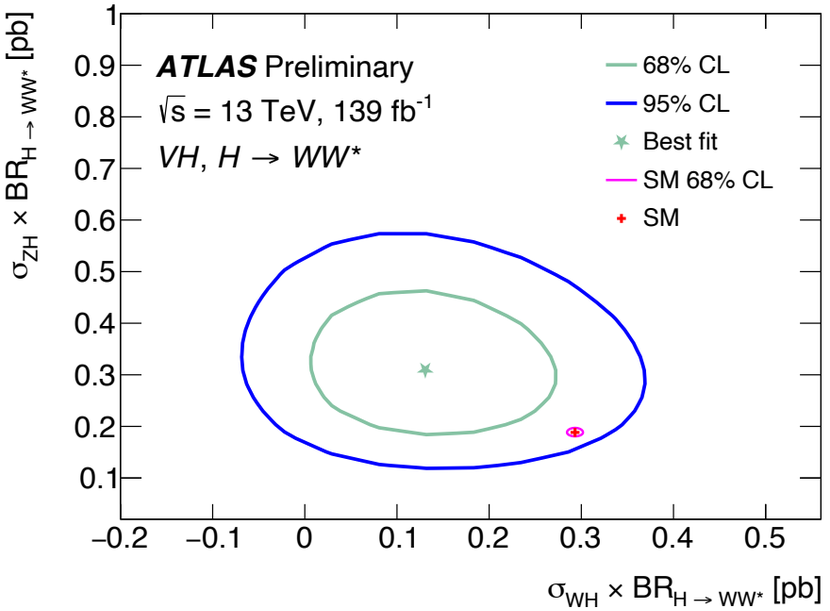

ATLAS-CONF-2022-067

4.6σ significance

VH production, $H \to b\bar{b}/c\bar{c}$

VH, $H \to bb$, STXS and EFT interpretation

- Observation for both WH and ZH productions
- Extend STXS to high p_T kinematics

Eur. Phys. J. C 81 (2021) 178

Phys. Lett. B 816 (2021) 136204

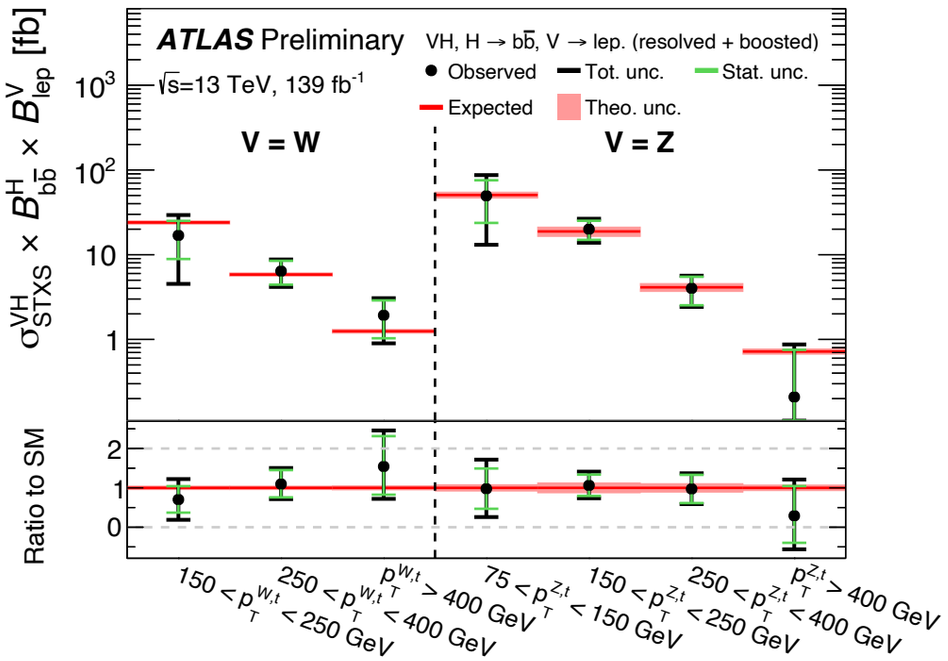

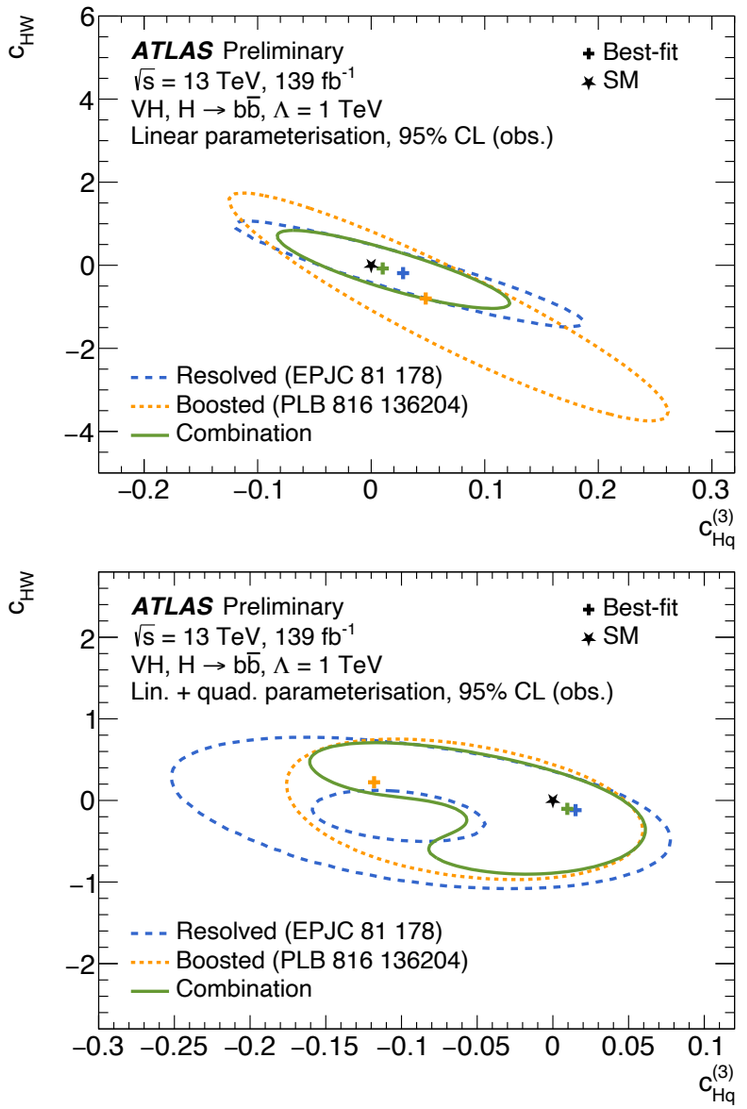

ATLAS-CONF-2021-051

VH, $H \to cc$, limit and interpretation

- Upper limit: 26 (31) times σ^{SM}
- Constraint on $|\kappa_c/\kappa_b| < 4.5$

NB: the number in () shows the expected value

26 (31)

Observed Expected

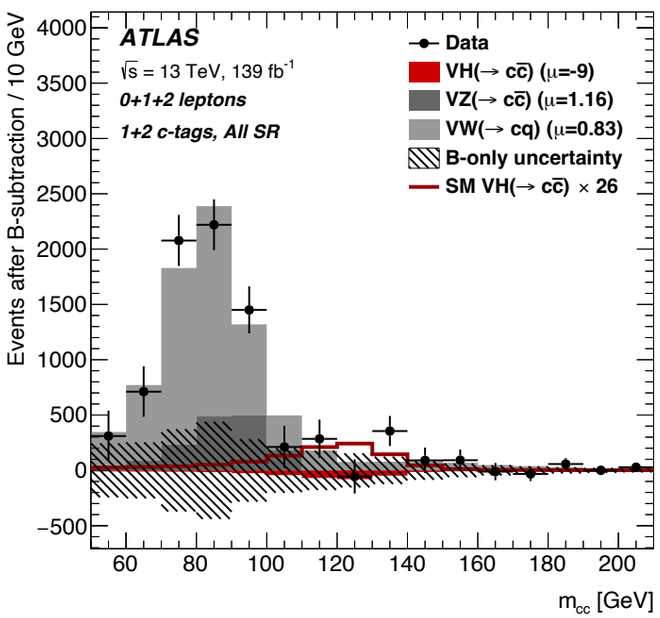

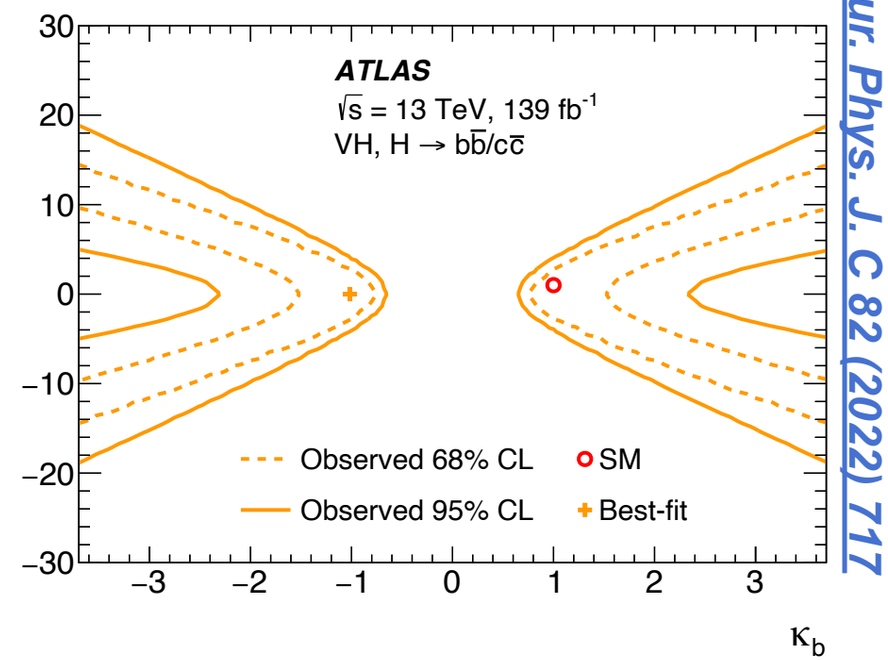

Eur. Phys. J. C 82 (2022) 717

VBF and *ttH* production, $H \to b\bar{b}$

VBF + photon

- Explore $H\gamma$ production

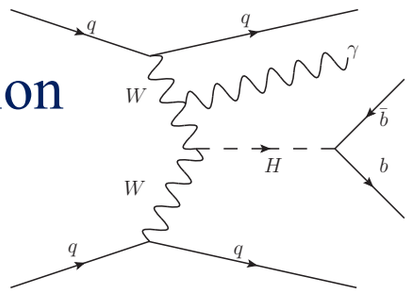

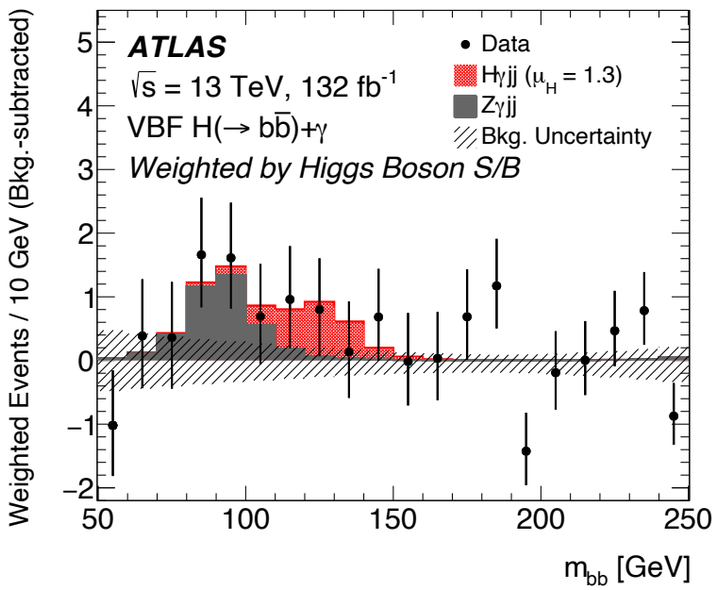

JHEP 03 (2021) 268

VBF production

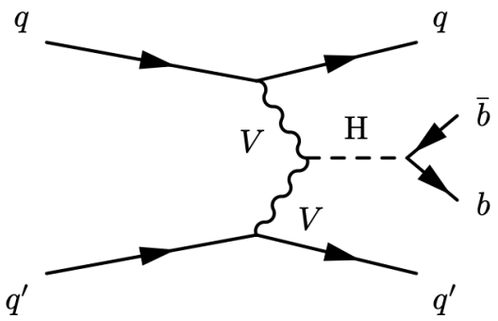

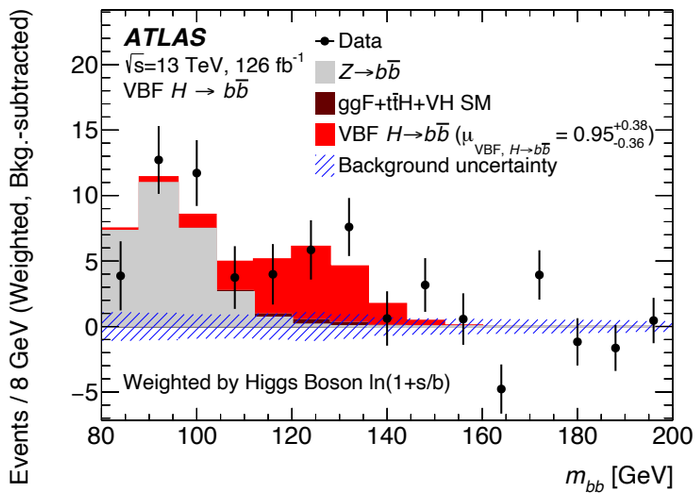

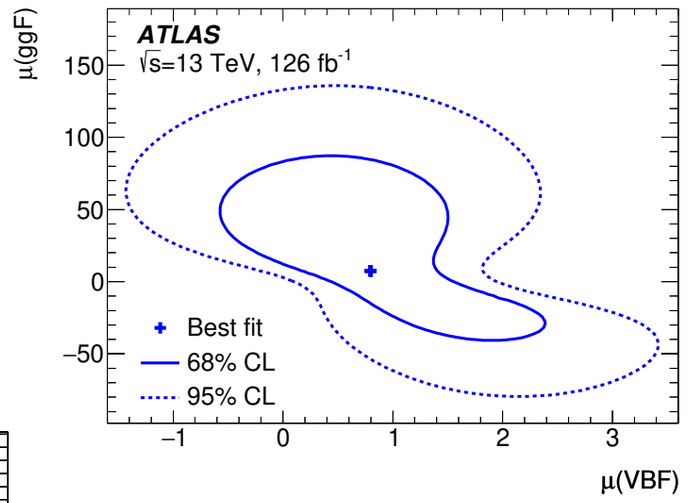

Eur. Phys. J. C. 81 (2021) 537

Combined results

(VBF and VBF + photon)

- Significance: 2.9 (2.9) σ ,
- $\mu = 0.99^{+0.36}_{-0.34}$,

ttH production, STXS measurements

- *ttH*: the best channel to direct observe the top-quark Yukawa coupling
- First STXS measurement on *ttH* production mode

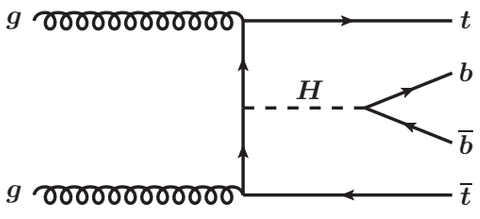

t-channel

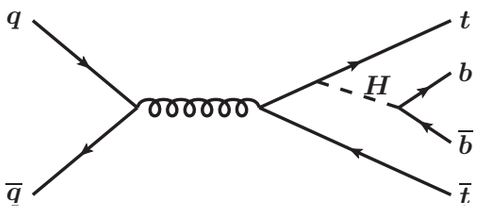

s-channel

Strength measured in different p_T^H bins

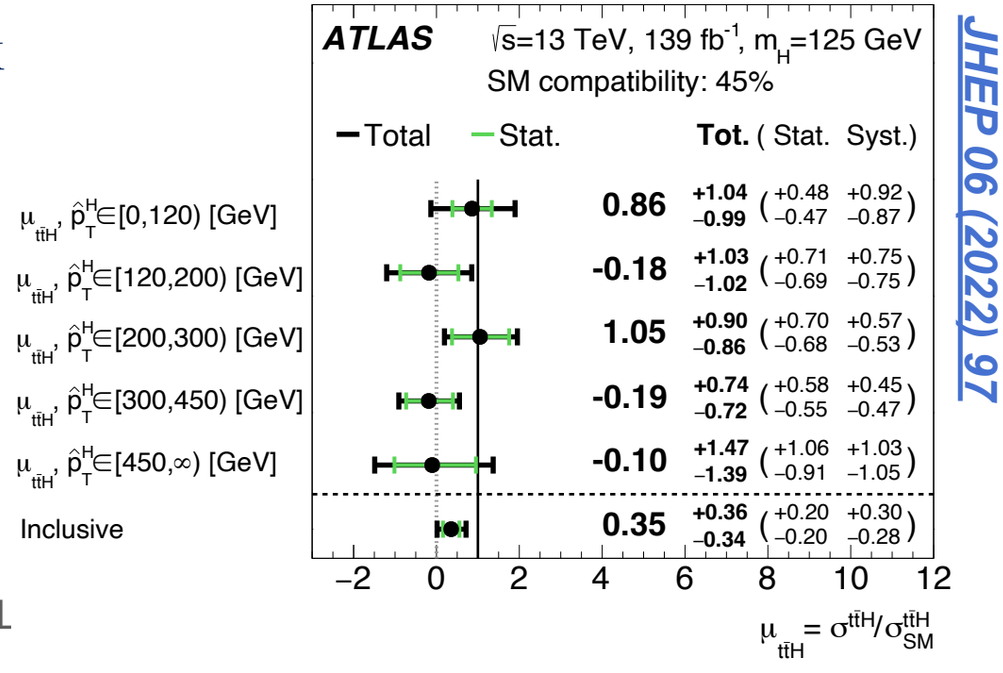

JHEP 06 (2022) 97

Higgs coupling with leptons

$H \to \tau\tau$ STXS, without V(lep)H production

- Significance: VBF 5.3(6.2)σ ggF 3.9(4.6)σ

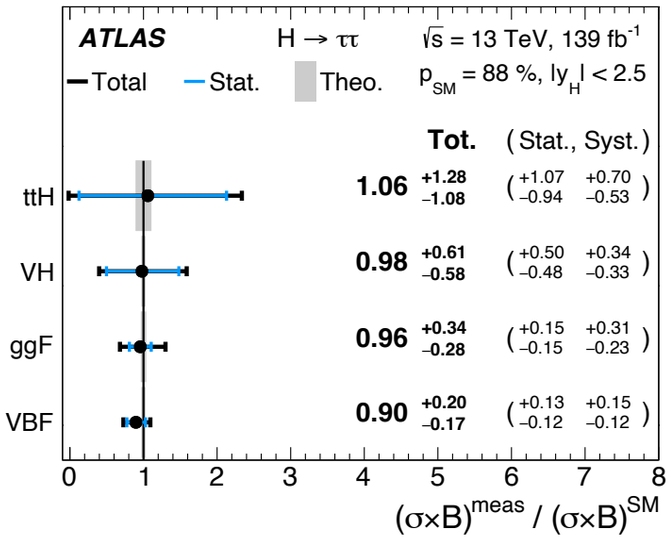

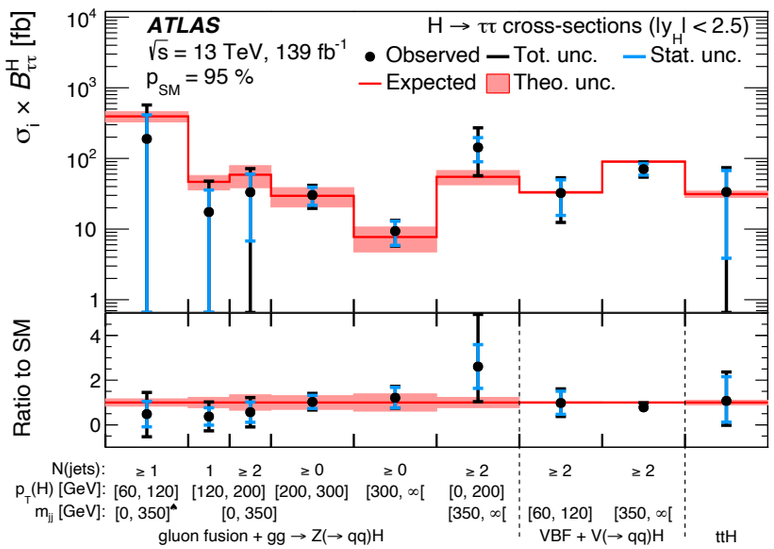

JHEP 08 (2022) 175

V(lep)H production, $H \to \tau\tau$

- Significance: 4.2(3.6)σ

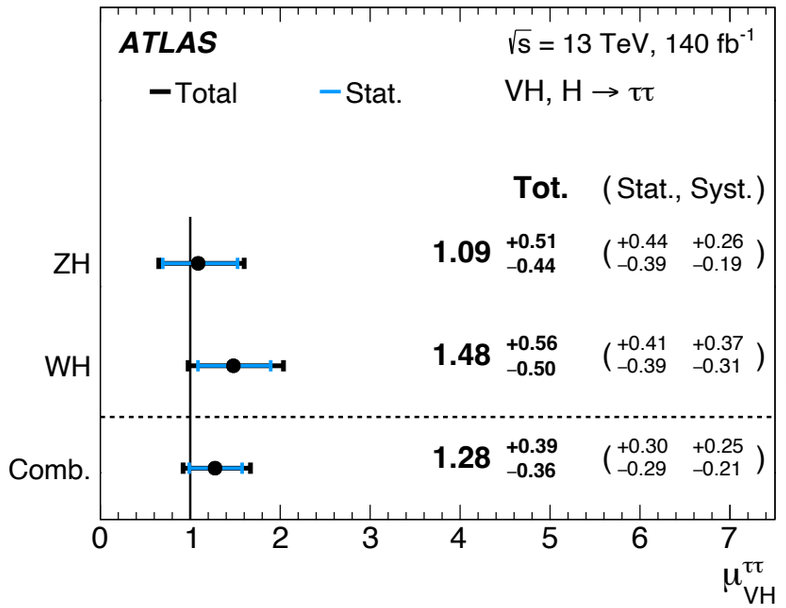

arXiv:2312.02394

$H \to \mu^+\mu^-$, Inclusive production mode

- Significance: 2.0(1.7)σ
- $\mu = 1.2 \pm 0.6$
- Using different categories targeting the different Higgs boson production modes

Phys. Lett. B 812 (2021) 135980

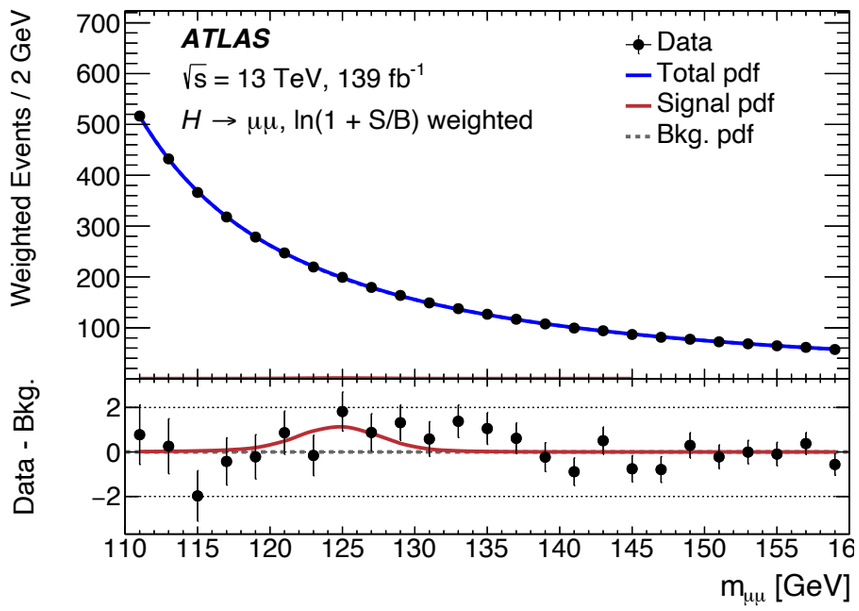

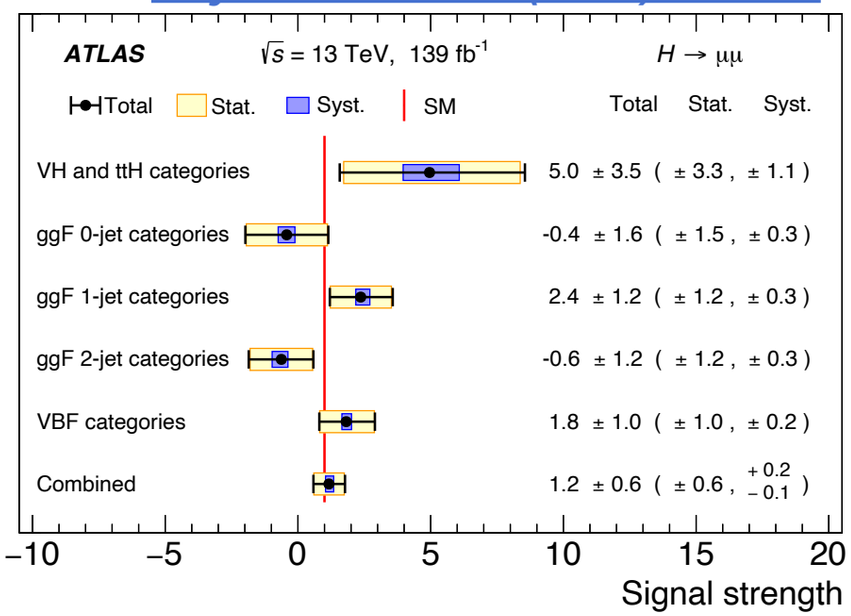

Evidence of $H \to Z\gamma$ and $\ell\ell + \gamma$ decay

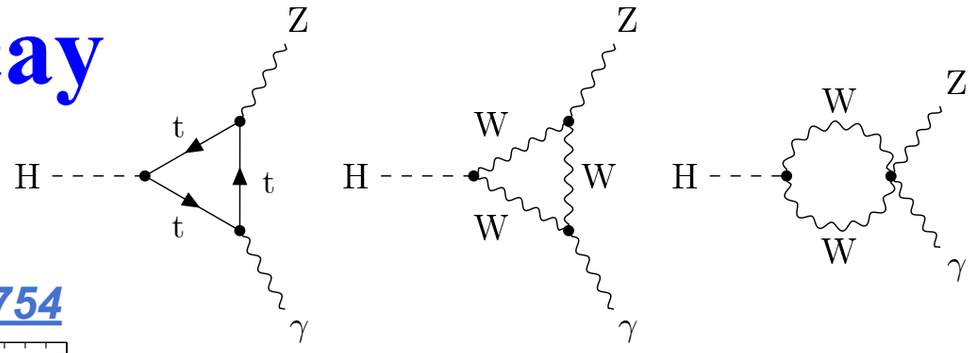

On shell Z + γ

ATLAS Run 2 results

- Signal strength: $\mu = 2.0^{+1.0}_{-0.9}$
- Significance: 2.2 (1.2)σ
- Upper limit: 3.6 (2.6) times σ^{SM}

ATLAS + CMS

- Signal strength: $\mu = 2.2 \pm 0.7$
- Significance: 3.4σ

Phys. Lett. B 809 (2020) 135754

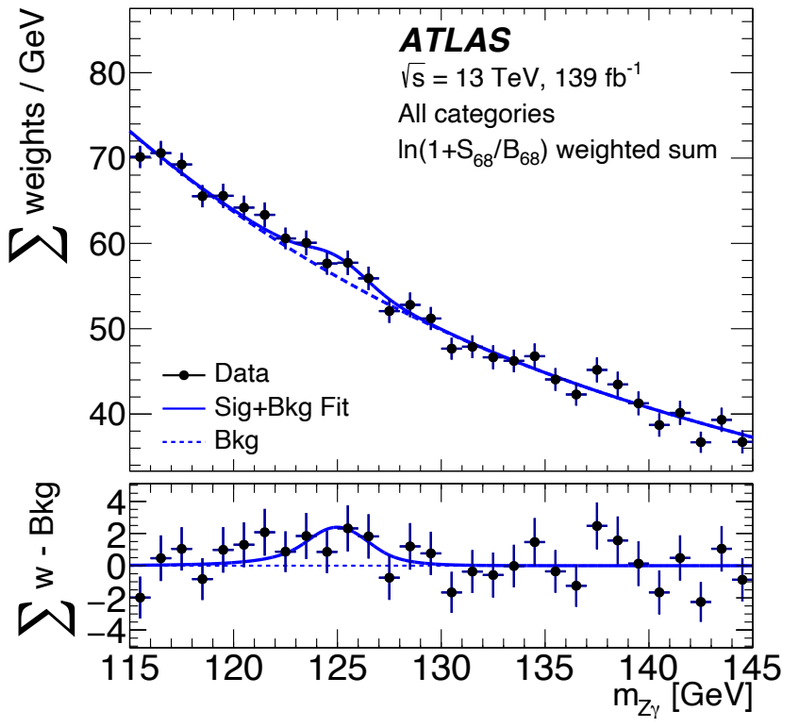

Phys. Rev. Lett. 132 (2024) 021803

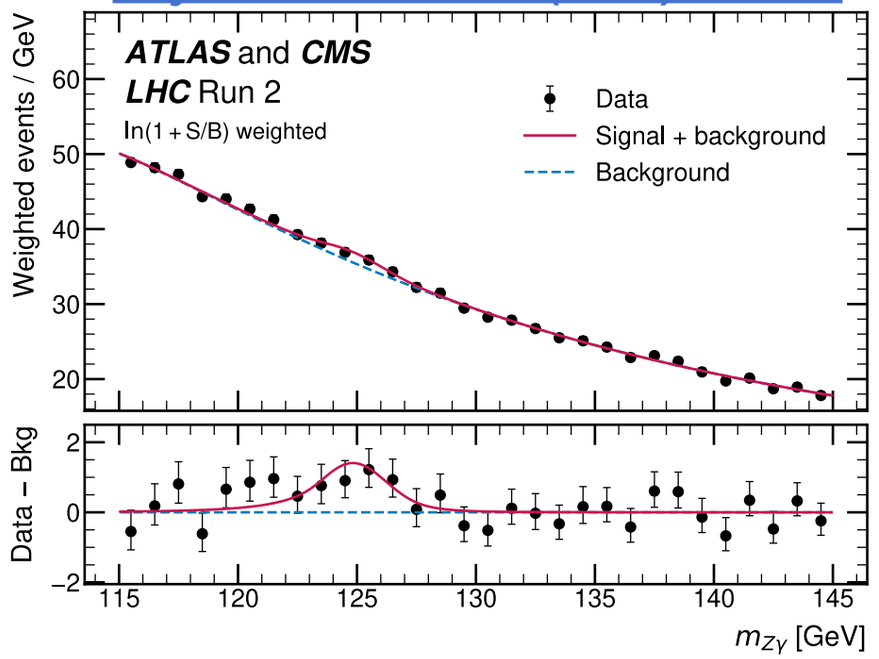

Low mass $\ell\ell + \gamma$

- Higgs decay to low mass dilepton system and a photon
- Require $m_{\ell\ell} < 30$ GeV

- Signal strength: $\mu = 1.5 \pm 0.5$
- Significance: 3.2 (2.1)σ

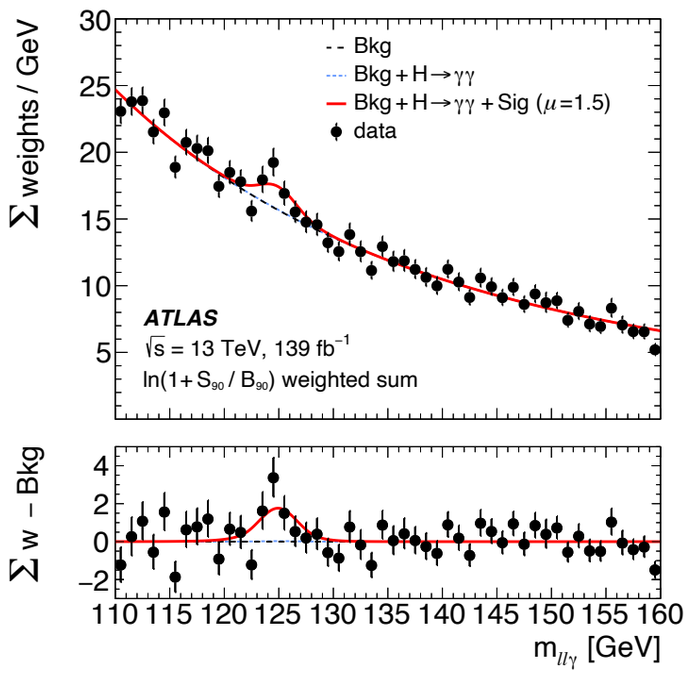

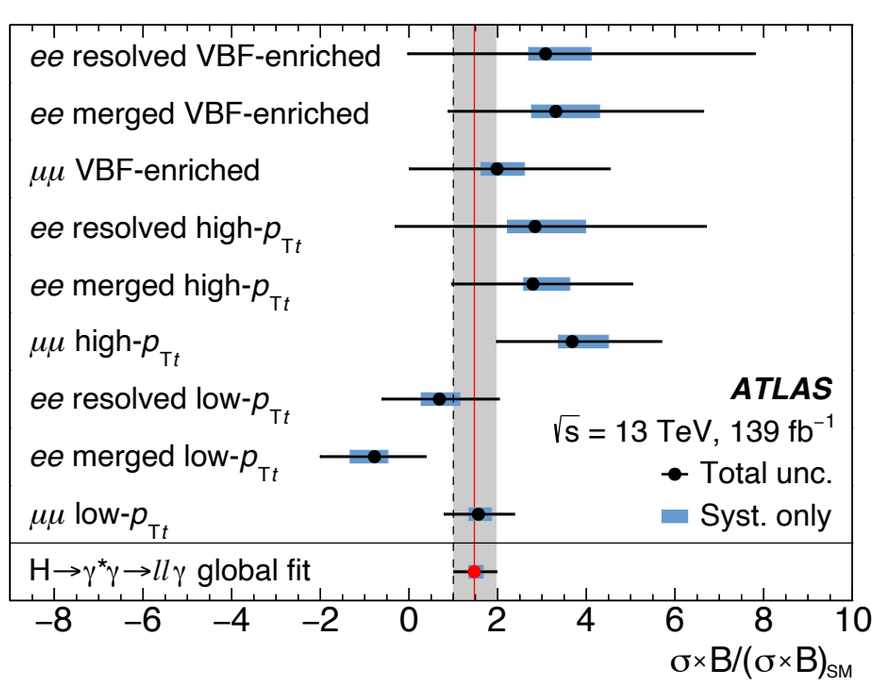

Phys. Lett. B 819 (2021) 136412

Higgs boson decay to invisible final states

- In the SM, the branching fraction to invisible final states is ~ 0.1%

  $H \to ZZ^* \to 4\nu$

- Invisible Higgs decay acts as a portal between dark sector and the SM sector

$$\kappa_H^2(\kappa, B_{inv}) = \frac{\Sigma_p B_p^{SM} \kappa_p^2}{1 - B_{inv}}$$

- All production modes are considered

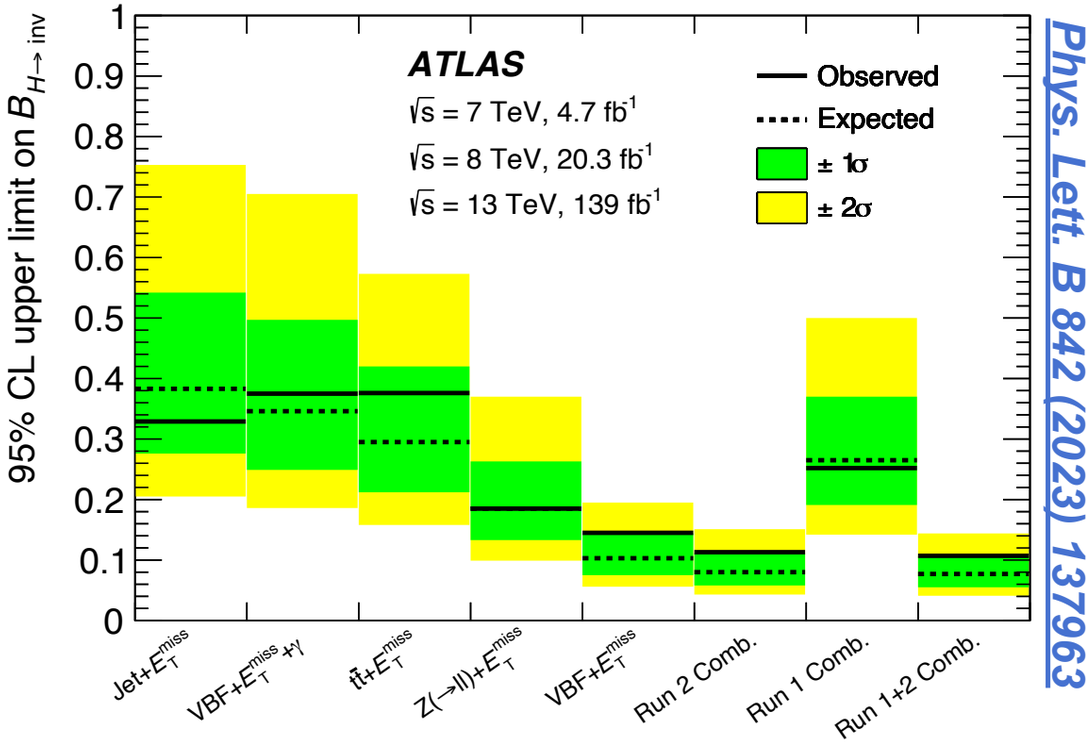

Combined Run 1 and Run 2 results:

- Observed branch ratio $B_{H\to inv.} = 0.04 \pm 0.04$
- 95% CL upper limit of $B_{H\to inv.}$: 0.107 (0.077)

Conclusion

- Many measurements and searches are presented from the ATLAS Run 2 data

$H \to \gamma\gamma$	High precision differential
$H \to ZZ$	XS and STXS
$H \to WW$	Toward high precision
$H \to bb$	
Higgs-top coupling (ttH)	
$H \to \tau\tau$	
$H \to Z\gamma$	Evidence (ATLAS + CMS)
$H \to cc$	To be discovered
$H \to \mu\mu$	

- Higgs measurements play an important role in BSM and new physics searches
- Interpretations with κ-framework and SMEFT
  No significant deviation is found
- The first Run 3 measurements are presented, more studies with Run 3 are ongoing

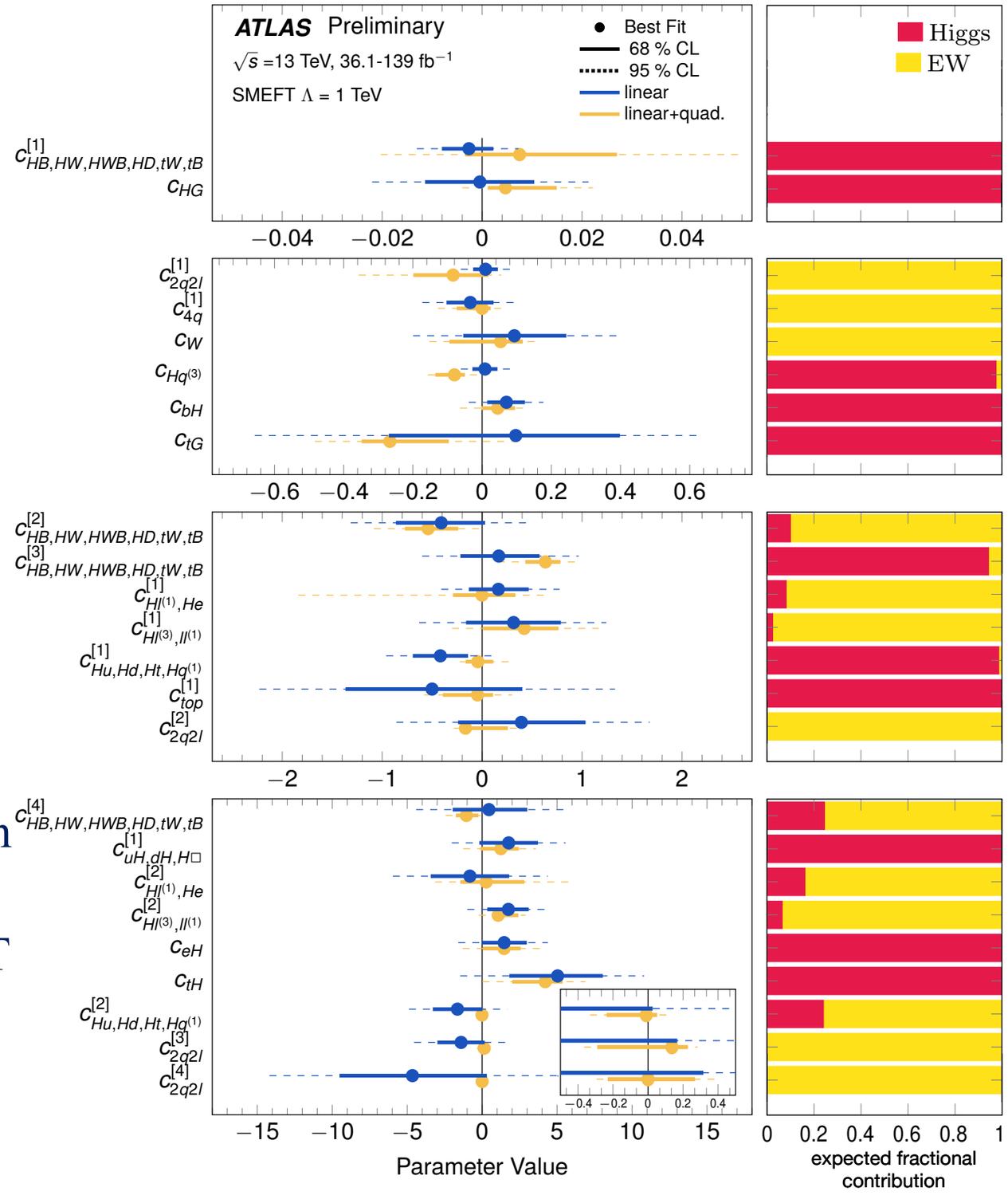

ATL-PHYS-PUB-2022-037

Constraints on Wilson coefficients from the combined ATLAS analysis

Back up

Higgs boson production and decay

- All the main Higgs boson production modes observed with > 5σ
- All the main decay modes are also observed

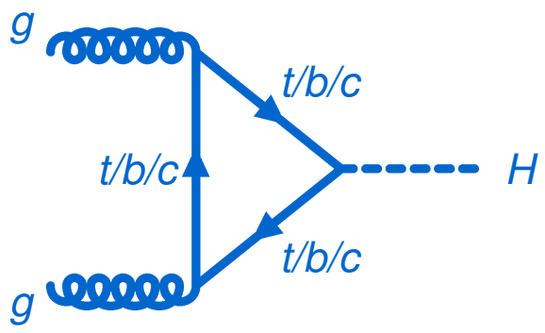

48.6 pb

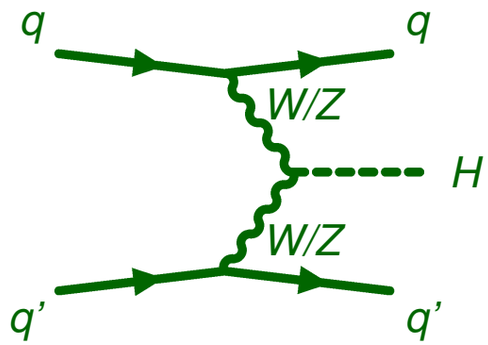

3.8 pb

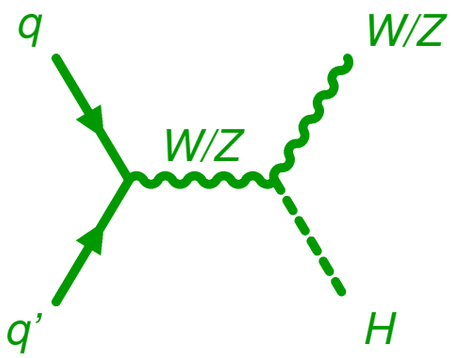

2.2 pb

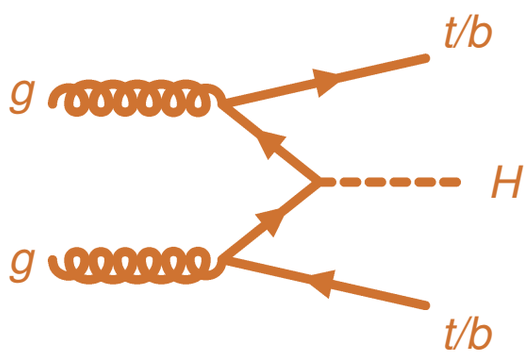

0.5 pb

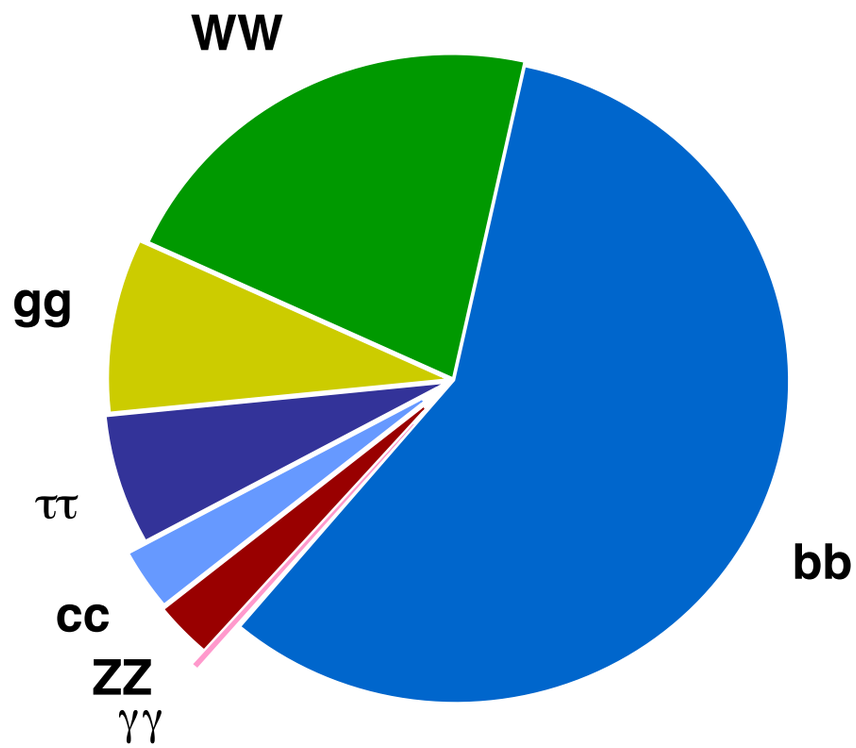

Compatibility of the correction measurements

[Nature 607, 52 (2022)]

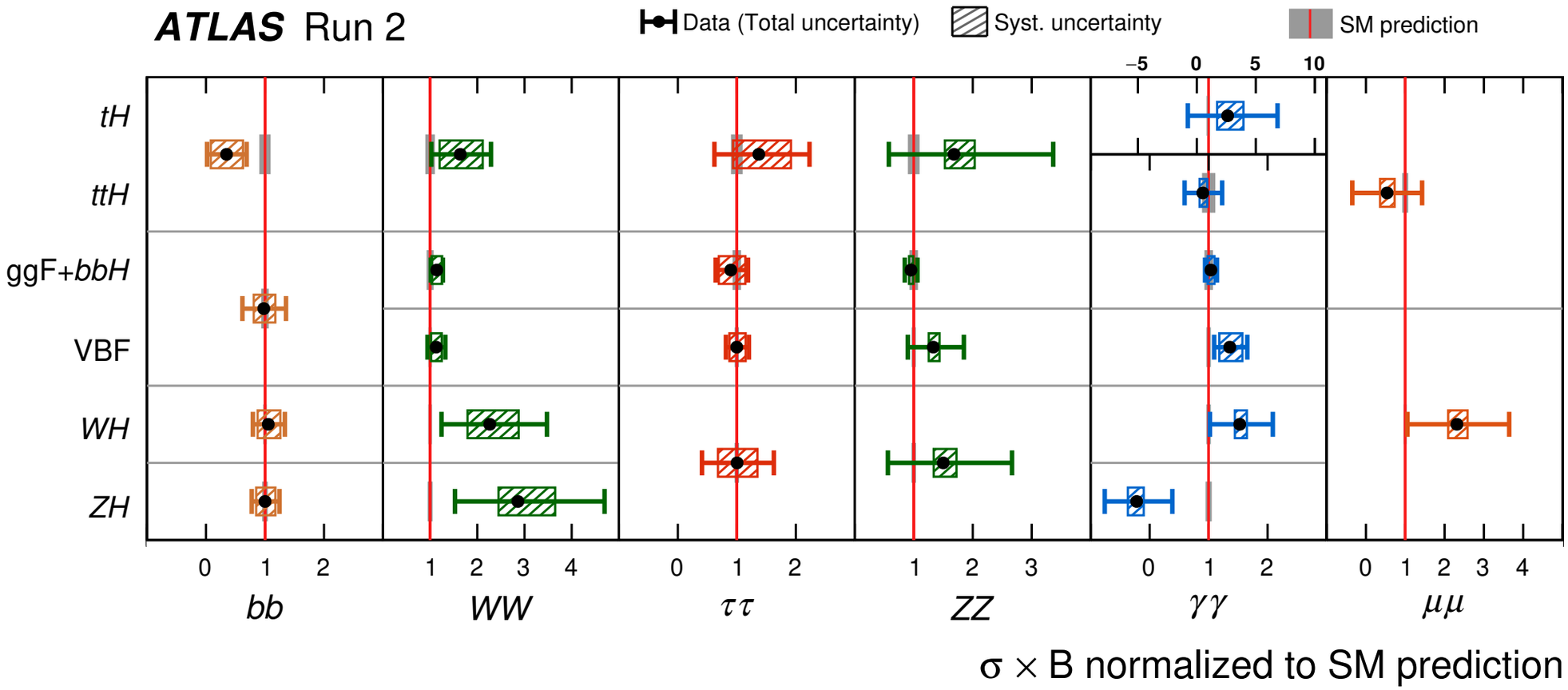

The p-value for compatibility of the measurement and the SM prediction is 72%

Fiducial and differential cross sections

Fiducial cross section measurements

- Fiducial region: defined to closely match to experimental acceptance

- Reduce model dependence by avoiding the extrapolation to the full phase space

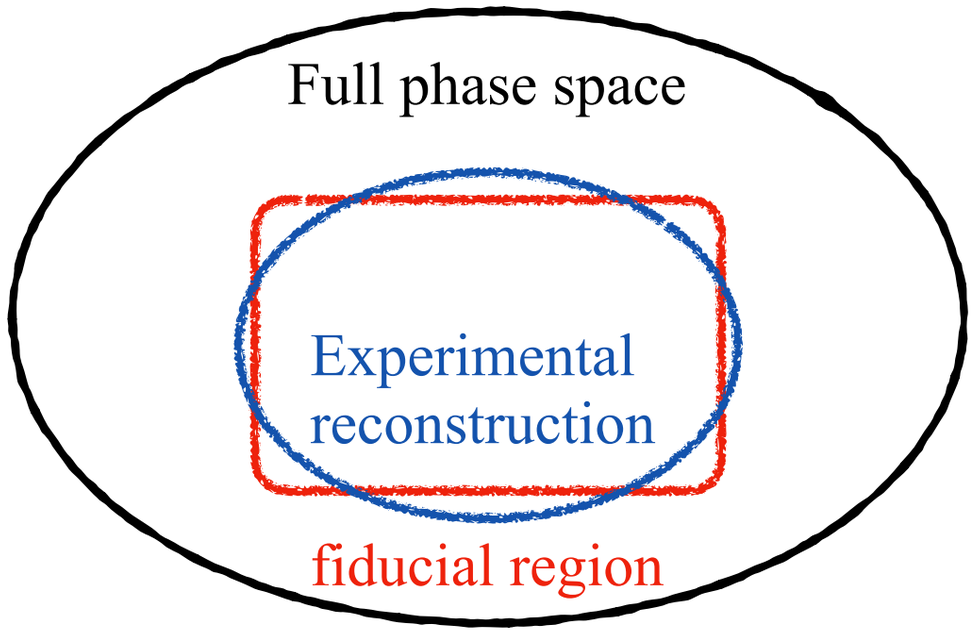

Differential cross section measurements

- Measure cross section in bins of some observables:
  $p_T^H, |y_H|, N_{jet} \cdots$

- The shape information provided by differential cross sections can be exploited for a range of further interpretations

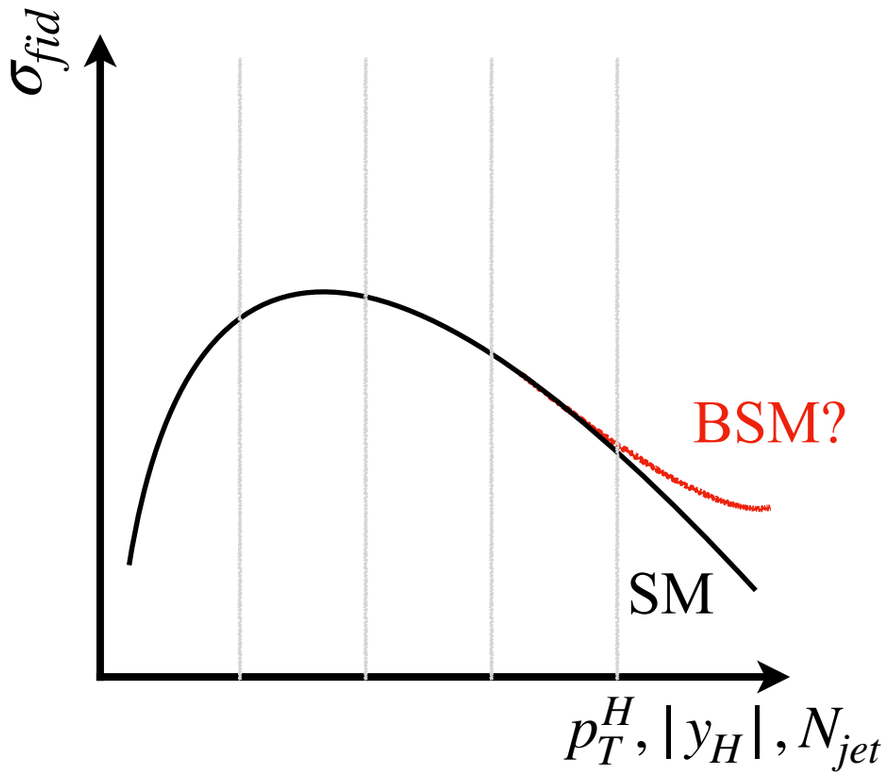

STXE stage 1.2

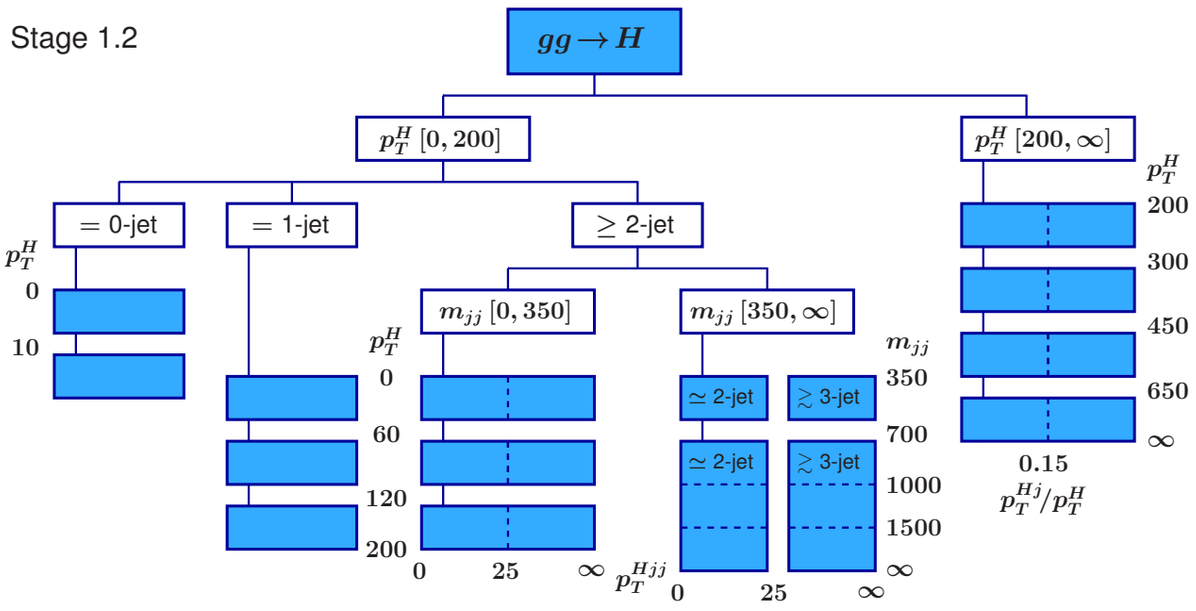

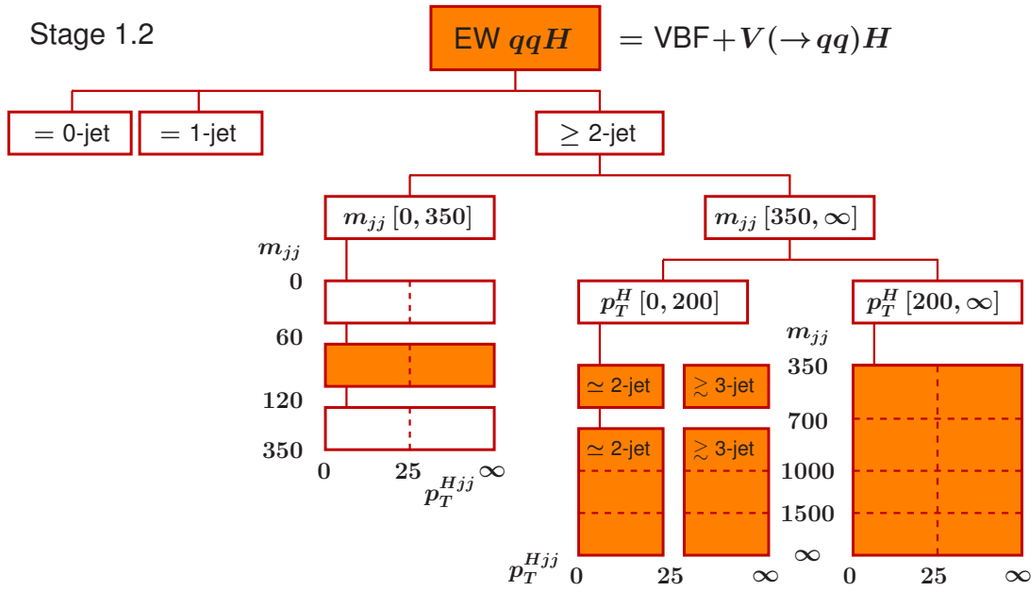

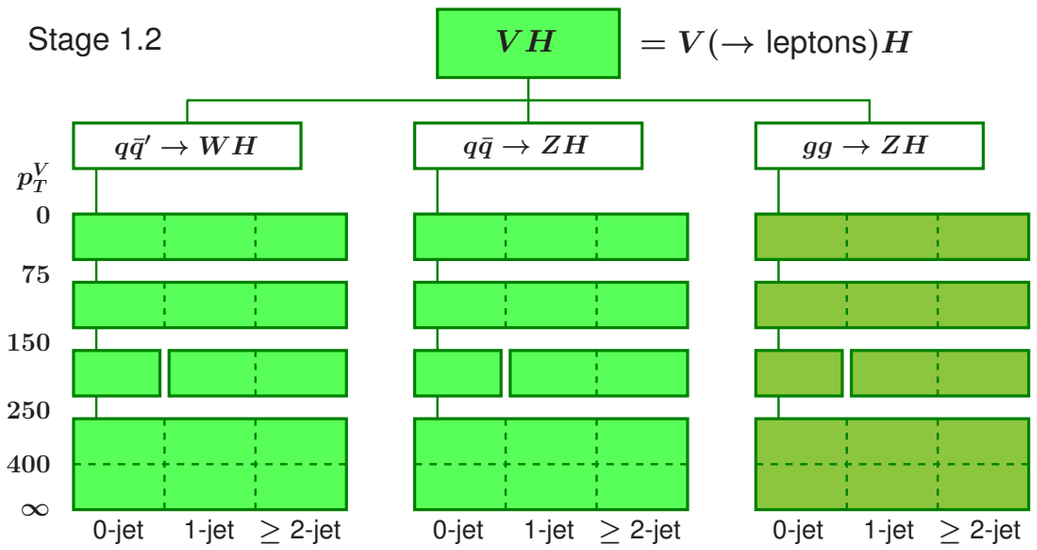

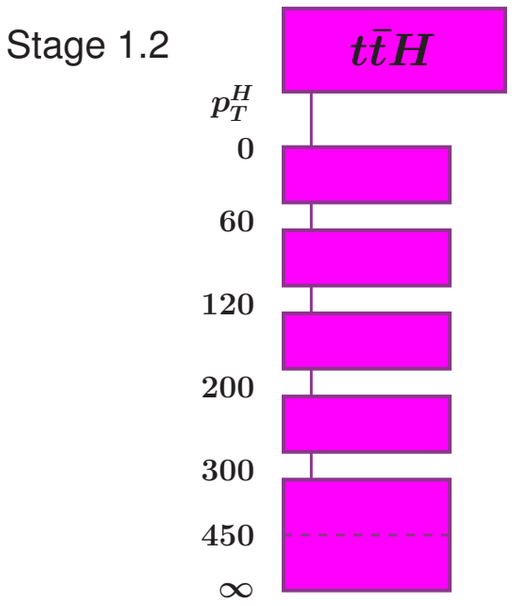

EFT coefficients

Wilson coefficient	Operator
c_H	$(H^\dagger H)^3$
$c_{H\Box}$	$(H^\dagger H)\Box(H^\dagger H)$
c_G	$f^{abc}G_\mu^{a\nu}G_\nu^{b\rho}G_\rho^{c\mu}$
c_W	$\epsilon^{IJK}W_\mu^{I\nu}W_\nu^{J\rho}W_\rho^{K\mu}$
c_{HDD}	$\left(H^\dagger D^\mu H\right)^*\left(H^\dagger D_\mu H\right)$
c_{HG}	$H^\dagger H\, G^A_{\mu\nu}G^{A\mu\nu}$
c_{HB}	$H^\dagger H\, B_{\mu\nu}B^{\mu\nu}$
c_{HW}	$H^\dagger H\, W^I_{\mu\nu}W^{I\mu\nu}$
c_{HWB}	$H^\dagger\tau^I H\, W^I_{\mu\nu}B^{\mu\nu}$
$c^{(1)}_{Hl,11}$	$(H^\dagger i\overleftrightarrow{D}_\mu H)(\bar{l}_1\gamma^\mu l_1)$
$c^{(1)}_{Hl,22}$	$(H^\dagger i\overleftrightarrow{D}_\mu H)(\bar{l}_2\gamma^\mu l_2)$
$c^{(1)}_{Hl,33}$	$(H^\dagger i\overleftrightarrow{D}_\mu H)(\bar{l}_3\gamma^\mu l_3)$
$c^{(3)}_{Hl,11}$	$(H^\dagger i\overleftrightarrow{D}^I_\mu H)(\bar{l}_1\tau^I\gamma^\mu l_1)$
$c^{(3)}_{Hl,22}$	$(H^\dagger i\overleftrightarrow{D}^I_\mu H)(\bar{l}_2\tau^I\gamma^\mu l_2)$
$c^{(3)}_{Hl,33}$	$(H^\dagger i\overleftrightarrow{D}^I_\mu H)(\bar{l}_3\tau^I\gamma^\mu l_3)$
$c_{He,11}$	$(H^\dagger i\overleftrightarrow{D}_\mu H)(\bar{e}_1\gamma^\mu e_1)$
$c_{He,22}$	$(H^\dagger i\overleftrightarrow{D}_\mu H)(\bar{e}_2\gamma^\mu e_2)$
$c_{He,33}$	$(H^\dagger i\overleftrightarrow{D}_\mu H)(\bar{e}_3\gamma^\mu e_3)$
$c^{(1)}_{Hq}$	$(H^\dagger i\overleftrightarrow{D}_\mu H)(\bar{q}\gamma^\mu q)$
$c^{(3)}_{Hq}$	$(H^\dagger i\overleftrightarrow{D}^I_\mu H)(\bar{q}\tau^I\gamma^\mu q)$
c_{Hu}	$(H^\dagger i\overleftrightarrow{D}_\mu H)(\bar{u}_p\gamma^\mu u_r)$
c_{Hd}	$(H^\dagger i\overleftrightarrow{D}_\mu H)(\bar{d}_p\gamma^\mu d_r)$
$c^{(1)}_{HQ}$	$(H^\dagger i\overleftrightarrow{D}_\mu H)(\bar{Q}\gamma^\mu Q)$
$c^{(3)}_{HQ}$	$(H^\dagger i\overleftrightarrow{D}^I_\mu H)(\bar{Q}\tau^I\gamma^\mu Q)$
c_{Ht}	$(H^\dagger i\overleftrightarrow{D}_\mu H)(\bar{t}\gamma^\mu t)$
c_{Hb}	$(H^\dagger i\overleftrightarrow{D}_\mu H)(\bar{b}\gamma^\mu b)$

Wilson coefficient	Operator
$c^{(1,1)}_{Qq}$	$(\bar{Q}\gamma_\mu Q)(\bar{q}\gamma^\mu q)$
$c^{(1,8)}_{Qq}$	$(\bar{Q}T^a\gamma_\mu Q)(\bar{q}T^a\gamma^\mu q)$
$c^{(3,1)}_{Qq}$	$(\bar{Q}\sigma^i\gamma_\mu Q)(\bar{q}\sigma^i\gamma^\mu q)$
$c^{(3,8)}_{Qq}$	$(\bar{Q}\sigma^iT^a\gamma_\mu Q)(\bar{q}\sigma^iT^a\gamma^\mu q)$
$c^{(3,1)}_{qq}$	$(\bar{q}\sigma^i\gamma_\mu q)(\bar{q}\sigma^i\gamma^\mu q)$
$c^{(1)}_{tu}$	$(\bar{t}\gamma_\mu t)(\bar{u}\gamma^\mu u)$
$c^{(8)}_{tu}$	$(\bar{t}T^a\gamma_\mu t)(\bar{u}T^a\gamma^\mu u)$
$c^{(1)}_{td}$	$(\bar{t}\gamma_\mu t)(\bar{d}\gamma^\mu d)$
$c^{(8)}_{td}$	$(\bar{t}T^a\gamma_\mu t)(\bar{d}T^a\gamma^\mu d)$
$c^{(1)}_{Qu}$	$(\bar{Q}\gamma_\mu Q)(\bar{u}\gamma^\mu u)$
$c^{(8)}_{Qu}$	$(\bar{Q}T^a\gamma_\mu Q)(\bar{u}T^a\gamma^\mu u)$
$c^{(1)}_{Qd}$	$(\bar{Q}\gamma_\mu Q)(\bar{d}\gamma^\mu d)$
$c^{(8)}_{Qd}$	$(\bar{Q}T^a\gamma_\mu Q)(\bar{d}T^a\gamma^\mu d)$
$c^{(1)}_{tq}$	$(\bar{q}\gamma_\mu q)(\bar{t}\gamma^\mu t)$
$c^{(8)}_{tq}$	$(\bar{q}T^a\gamma_\mu q)(\bar{t}T^a\gamma^\mu t)$
$c_{eH,22}$	$(H^\dagger H)(\bar{l}_2e_2H)$
$c_{eH,33}$	$(H^\dagger H)(\bar{l}_3e_3H)$
c_{uH}	$(H^\dagger H)(\bar{q}Y_u^\dagger u\widetilde{H})$
c_{tH}	$(H^\dagger H)(\bar{Q}\widetilde{H}t)$
c_{bH}	$(H^\dagger H)(\bar{Q}Hb)$
c_{tG}	$(\bar{Q}\sigma^{\mu\nu}T^At)\widetilde{H}\, G^A_{\mu\nu}$
c_{tW}	$(\bar{Q}\sigma^{\mu\nu}t)\tau^I\widetilde{H}\, W^I_{\mu\nu}$
c_{tB}	$(\bar{Q}\sigma^{\mu\nu}t)\widetilde{H}\, B_{\mu\nu}$
$c_{ll,1221}$	$(\bar{l}_1\gamma_\mu l_2)(\bar{l}_2\gamma^\mu l_1)$

Observed value and uncertainties of EFT coefficients

Parameter	Value	σ_{tot}	σ_{stat}	σ_{syst}	$\sigma^{\text{exp}}_{\text{syst}}$	$\sigma^{\text{th.sig}}_{\text{syst}}$	$\sigma^{\text{th.bkg}}_{\text{syst}}$
$c_{eH,22}$	-0.0002	0.0028	0.0026	0.0009	0.0006	0.00049	$^{+0.0003}_{-0.0005}$
$c_{eH,33}$	0.019	0.016	0.011	0.011	0.008	0.006	0.005
$c^{(3)}_{Hq}$	0.039	0.040	0.034	0.021	0.015	$^{+0.011}_{-0.005}$	0.012
c_{bH}	0.055	$^{+0.039}_{-0.058}$	$^{+0.032}_{-0.045}$	$^{+0.023}_{-0.037}$	$^{+0.014}_{-0.022}$	0.015	$^{+0.013}_{-0.025}$
$e^{[1]}_{\text{ggF}}$	0.0003	0.0039	0.0029	0.0026	0.0013	0.0021	$^{+0.0013}_{-0.0008}$
$e^{[2]}_{\text{ggF}}$	-0.07	0.38	0.29	0.25	0.13	0.11	0.18
$e^{[3]}_{\text{ggF}}$	5.5	7.1	5.8	4.00	2.71	$^{+2.8}_{-2.1}$	1.6
$e^{[1]}_{H\gamma\gamma,Z\gamma}$	0.0048	0.0043	0.0034	0.0026	0.0017	0.0015	0.0012
$e^{[2]}_{H\gamma\gamma,Z\gamma}$	-0.042	0.041	0.037	$^{+0.015}_{-0.022}$	0.014	$^{+0.006}_{-0.011}$	$^{+0.006}_{-0.010}$
$e^{[3]}_{H\gamma\gamma,Z\gamma}$	-0.47	0.62	0.51	0.35	0.24	0.20	0.16
$e^{[1]}_{ZH}$	-0.14	0.34	0.29	0.19	0.16	0.09	$^{+0.08}_{-0.11}$
$e^{[2]}_{ZH}$	3.7	3.9	3.3	2.1	1.6	0.9	1.0
$e^{[3]}_{ZH}$	1.8	8.5	7.2	4.5	3.4	2.2	2.0
$e^{[4]}_{ZH}$	4.8	9.8	8.2	5.2	4.0	2.5	2.2
$e^{[1]}_{\text{ttH}}$	-0.65	0.84	0.64	0.54	0.31	0.17	0.41
$e^{[2]}_{\text{ttH}}$	-0.05	3.7	2.8	2.4	0.94	$^{+0.3}_{-0.6}$	2.2
$e^{[3]}_{\text{ttH}}$	8.6	$^{+13.4}_{-9.2}$	$^{+12.1}_{-8.8}$	$^{+5.73}_{-2.91}$	$^{+3.9}_{-2.1}$	$^{+3.8}_{-1.5}$	$^{+2.0}_{-1.2}$
$e^{[1]}_{\text{glob}}$	0.13	$^{+0.83}_{-0.57}$	$^{+0.57}_{-0.42}$	$^{+0.60}_{-0.38}$	$^{+0.30}_{-0.20}$	$^{+0.42}_{-0.29}$	$^{+0.29}_{-0.17}$
$e^{[1]}_{Hllll}$	-0.349	1.1	0.76	0.74	0.44	0.38	0.46

arXiv:2402.05742

VBF *WH* production

arXiv:2402.00426

- To determine the ratio between Higgs coupling to W and Z : $\lambda_{WZ} = \kappa_W/\kappa_Z$
- Based on other results, $|\lambda_{WZ}|$ is constrained around 1, but the sign is not determined
- The interference between the two diagrams :
  - Destructive for SM, but constructive for negative λ_{WZ}

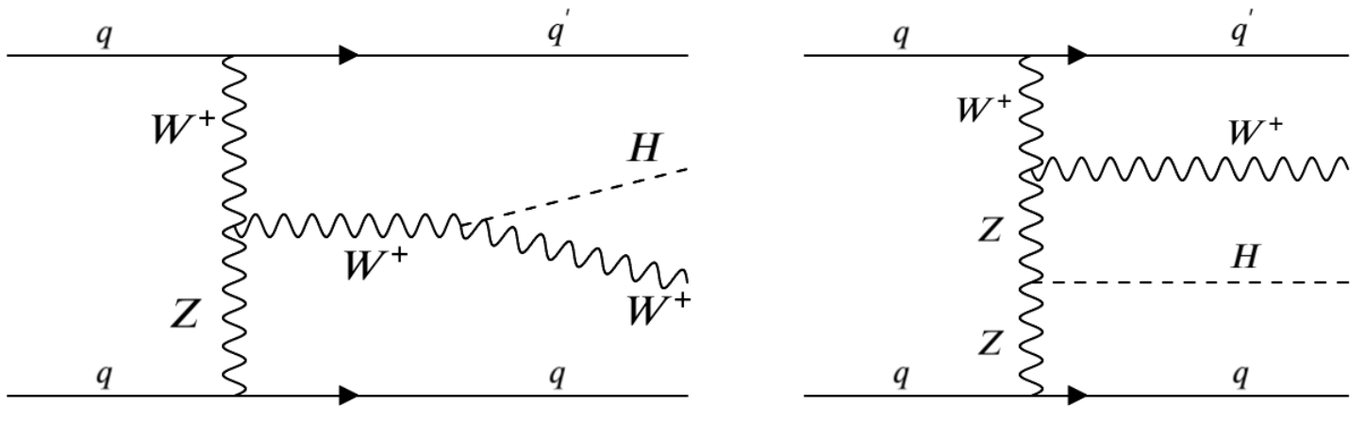

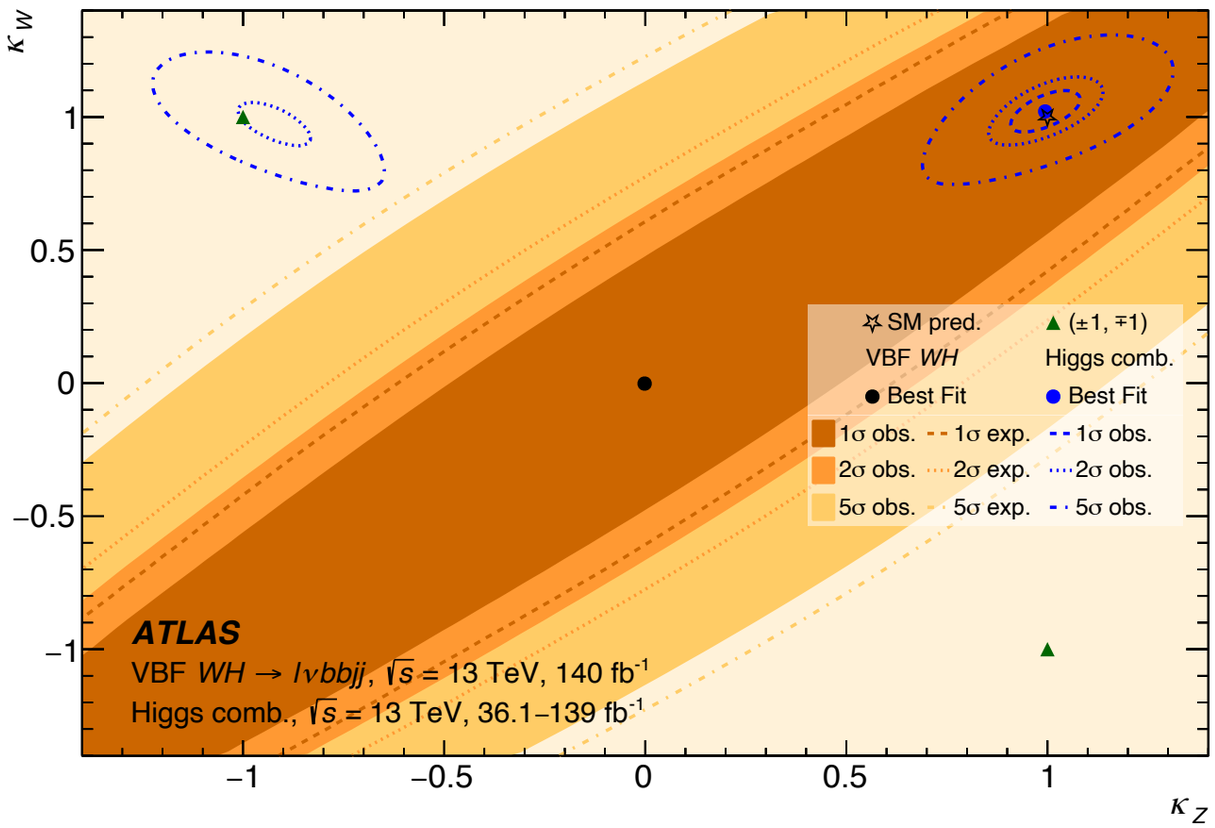

STXS $H \to ZZ^* \to 4\ell$ and $H \to \gamma\gamma$

[Eur. Phys. J. C 80 (2020) 957]

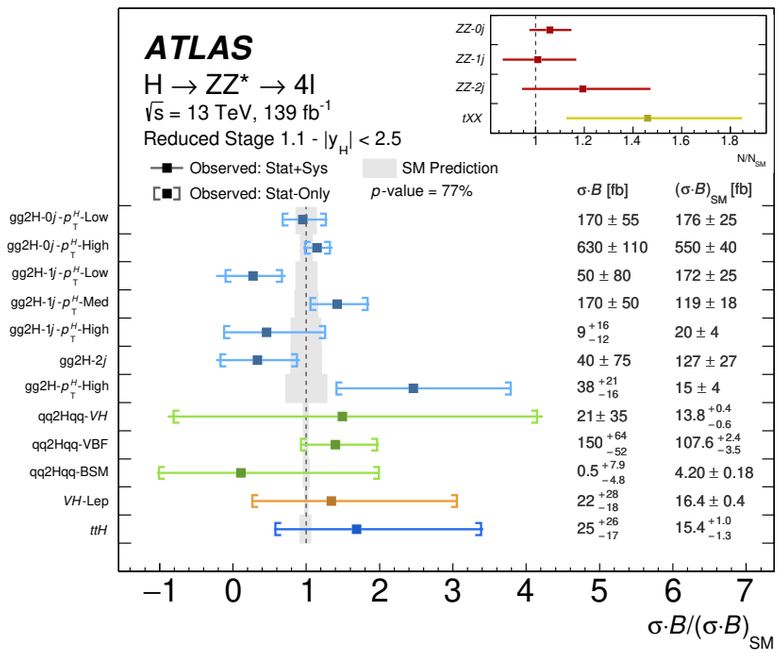

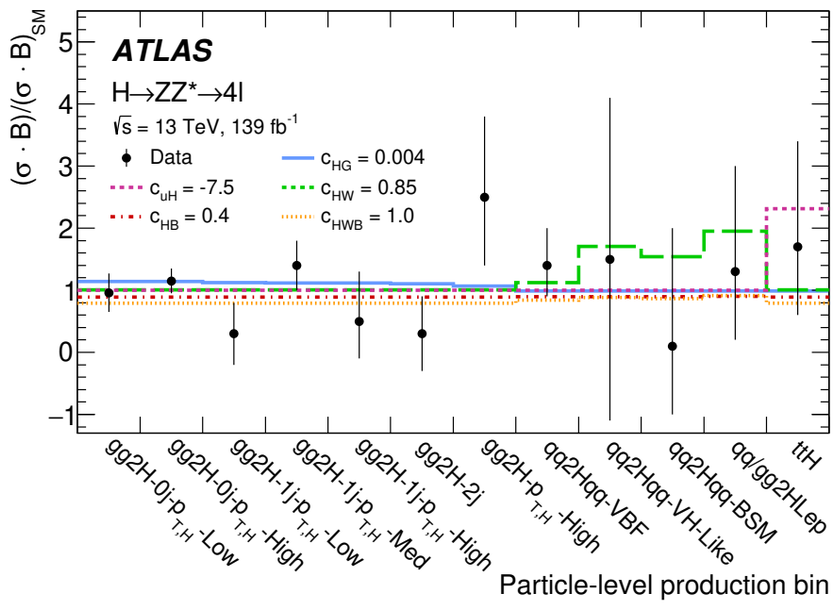

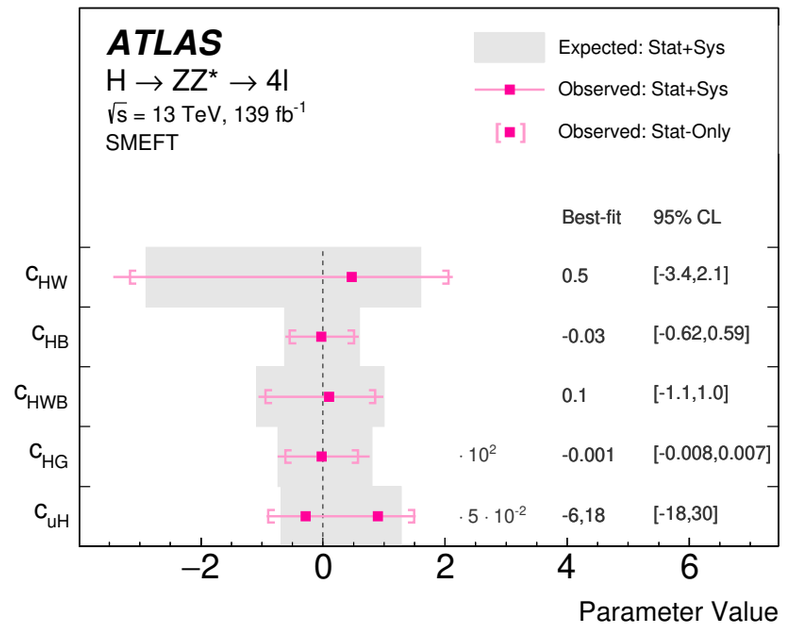

[JHEP 07 (2023) 088]

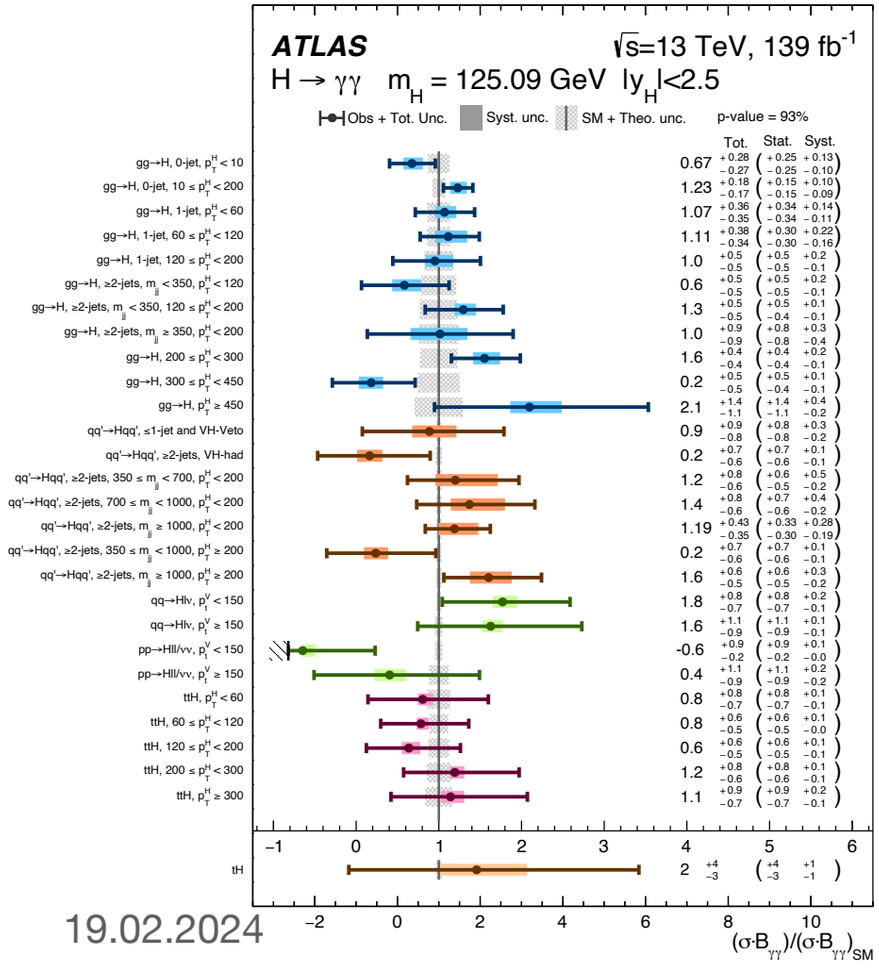

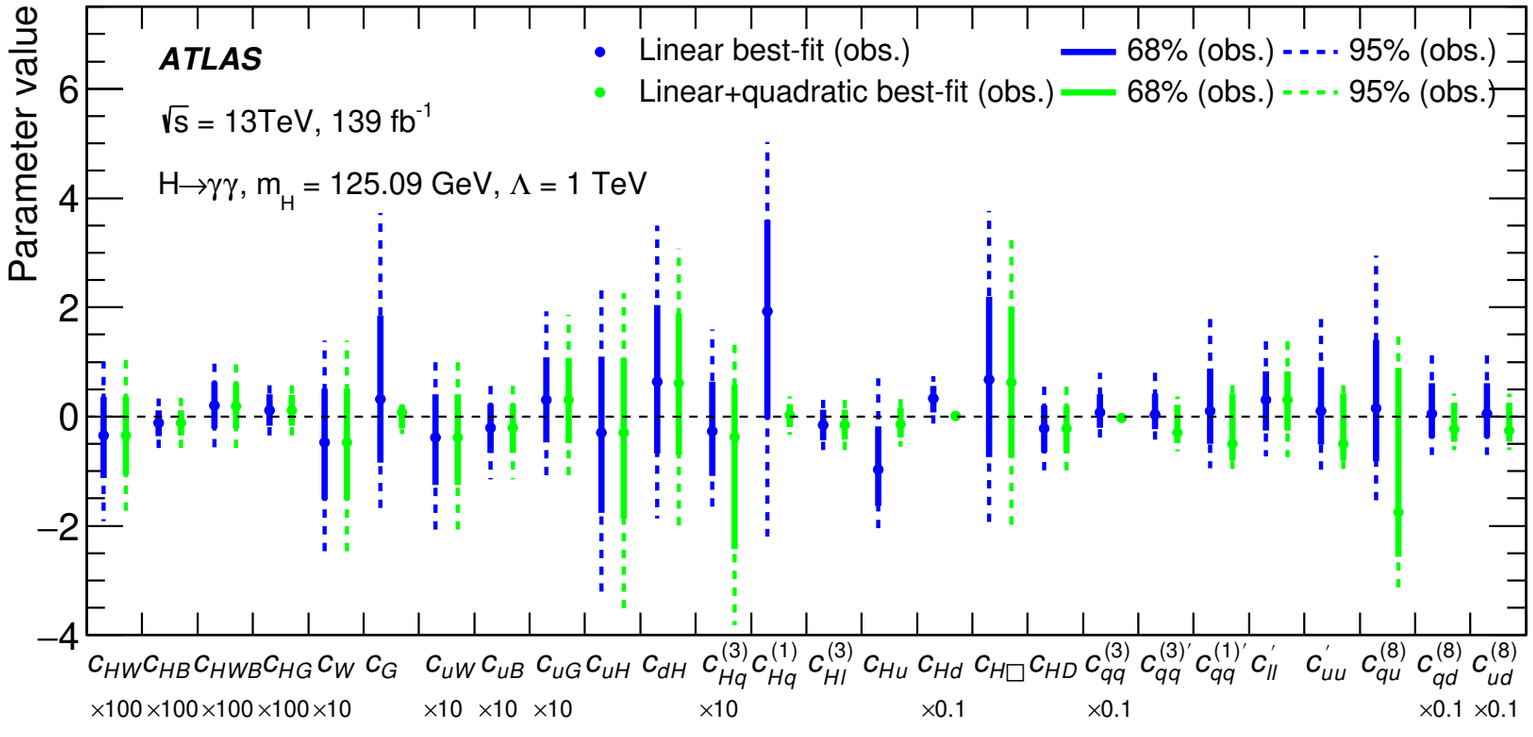

$H \rightarrow WW^*$ Cross-section measurement

- ggF and VBF production, $e\nu\mu\nu$ final states
- Simplified Template Cross Sections in a total of 11 kinematical fiducial regions

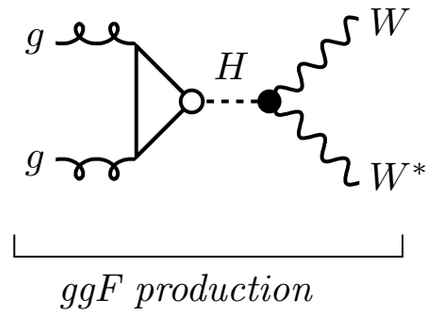

ggF production

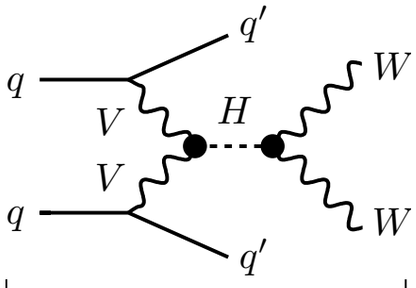

VBF production

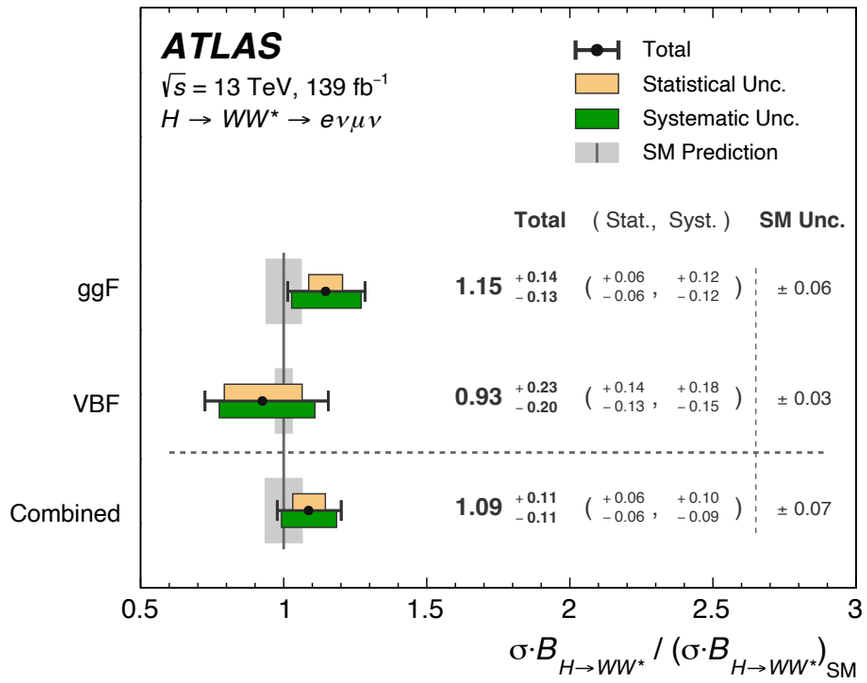

[Phys. Rev. D 108 (2023) 032005]

$$\sigma_{ggF} \cdot \mathscr{B}_{H\rightarrow WW^*} = 12.0 \pm 1.4\ pb$$

$$\sigma_{VBF} \cdot \mathscr{B}_{H\rightarrow WW^*} = 0.75^{+0.19}_{-0.16}\ pb$$

- VH production, $\ell\nu\ell\nu$ & $\ell\nu jj$final states [ATLAS-CONF-2022-067]

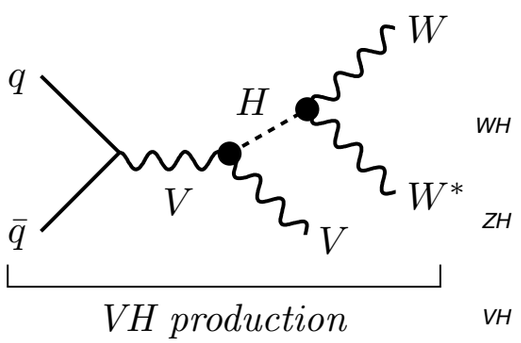

VH production

4.6σ significance

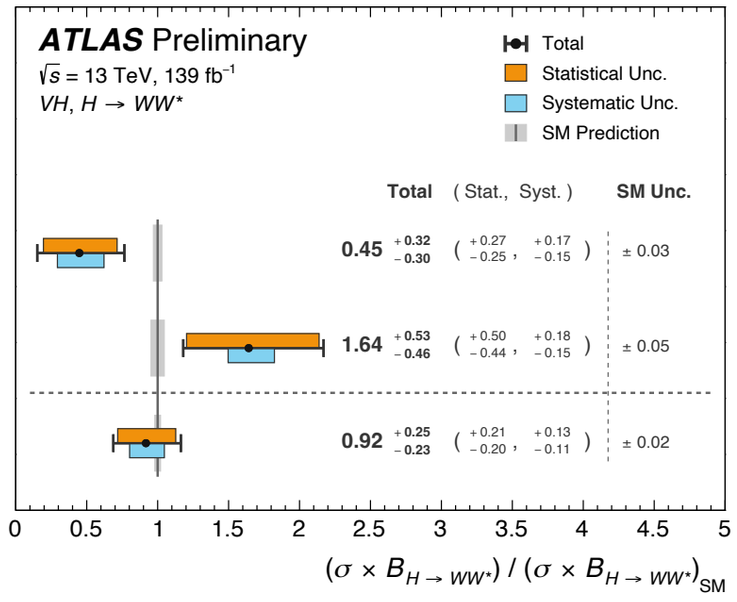

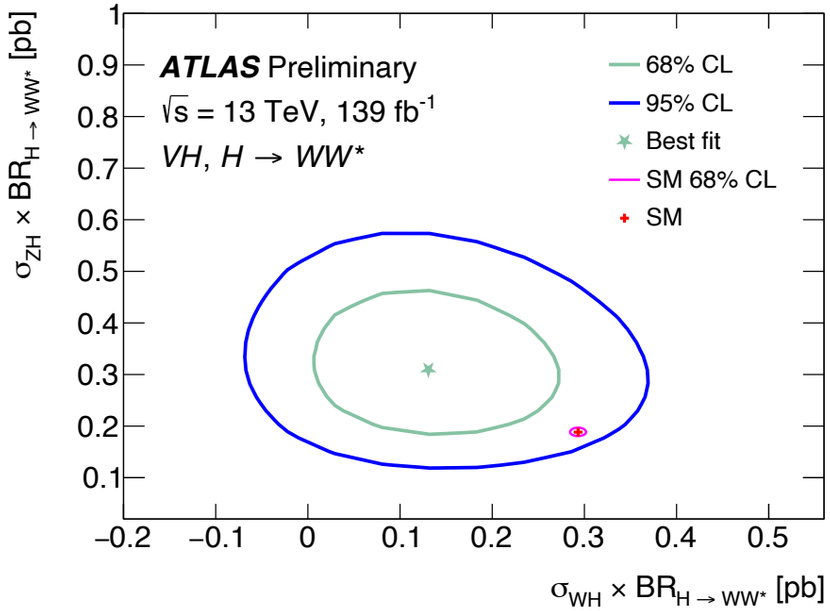

$H \to WW^* \to e\nu\mu\nu$ differential cross- section

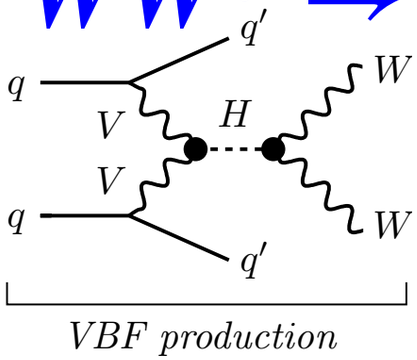

VBF production

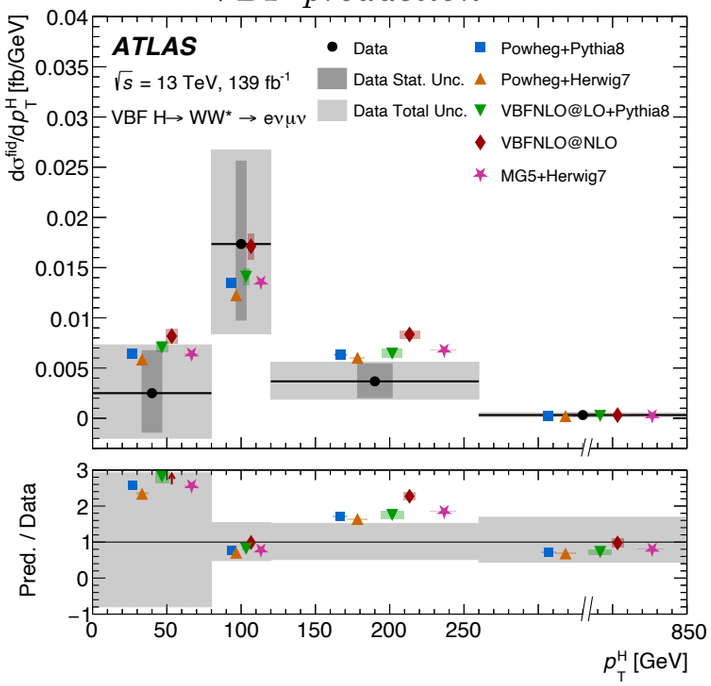

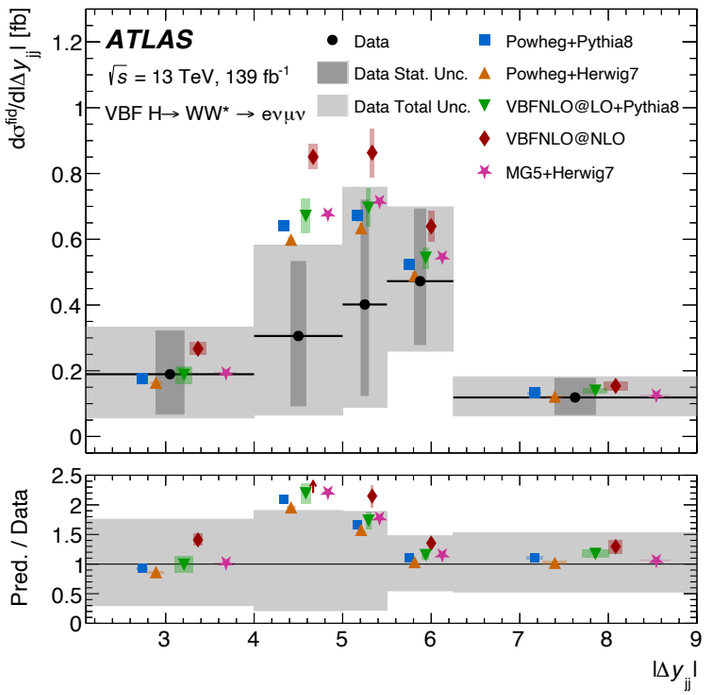

[Phys. Rev. D 108 (2023) 072003](#)

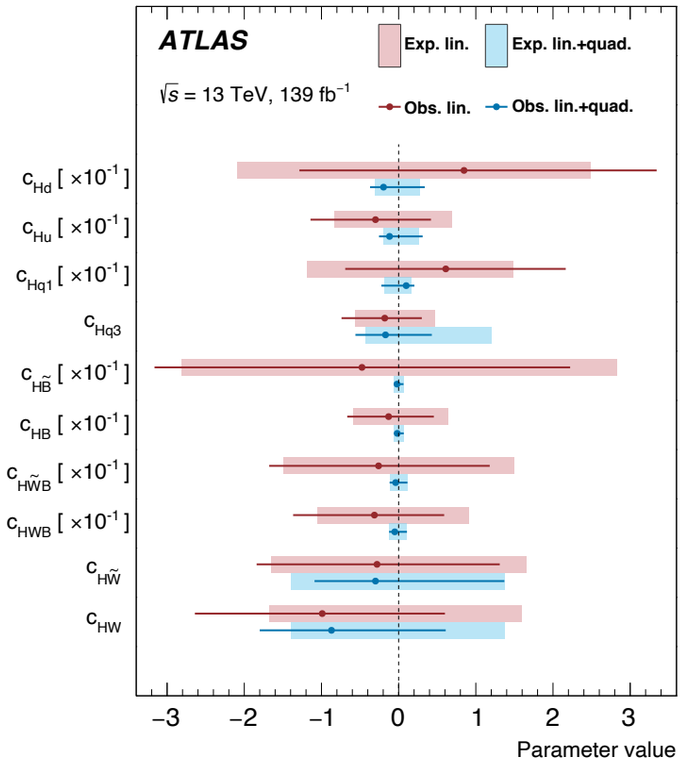

[Eur. Phys. J. C 83 (2023) 774](#)

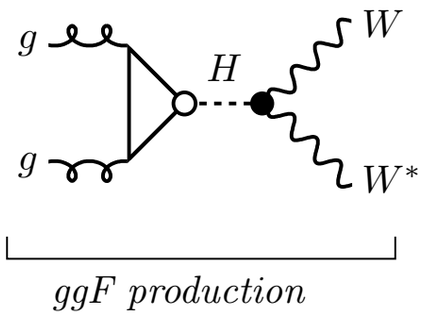

ggF production

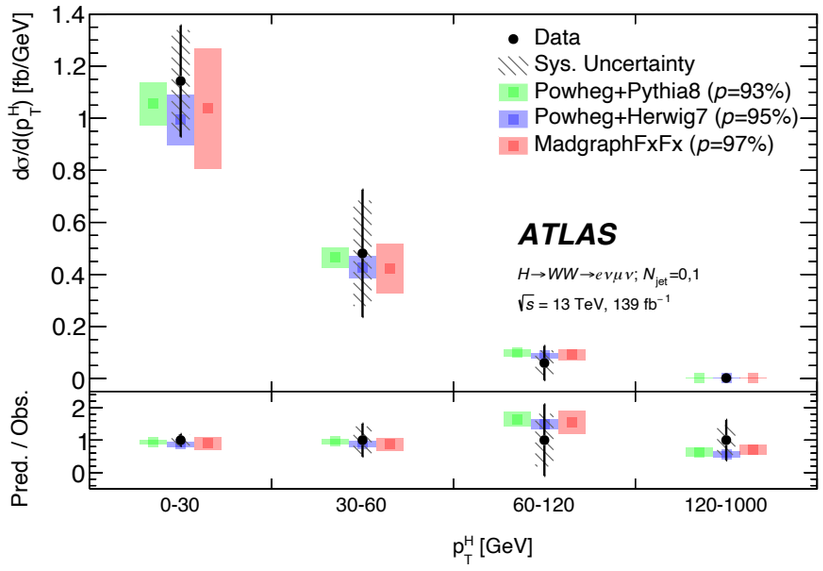

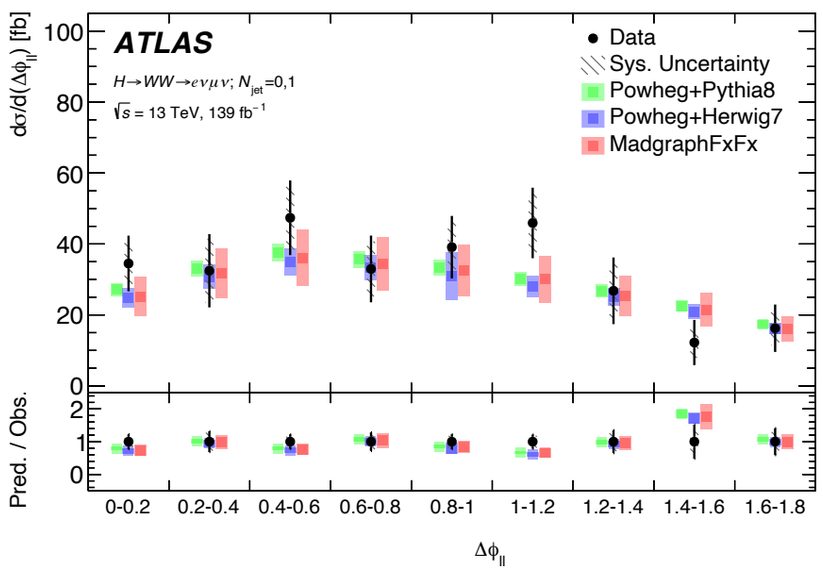

$VH(H \to b\bar{b})$ 0 lepton fiducial cross section

ATLAS-CONF-2022-015

- $H \to b\bar{b}$: largest branch ratio but complex background
- First fully fiducial measurement in $H \to b\bar{b} + E_T^{miss}$ final state
- Based on Run-2 resolved $VH(H \to b\bar{b})$ analysis Eur. Phys. J. C 81 (2021) 178

Background constraint

1L channel constrains top and W background

2L channel constrains Z background

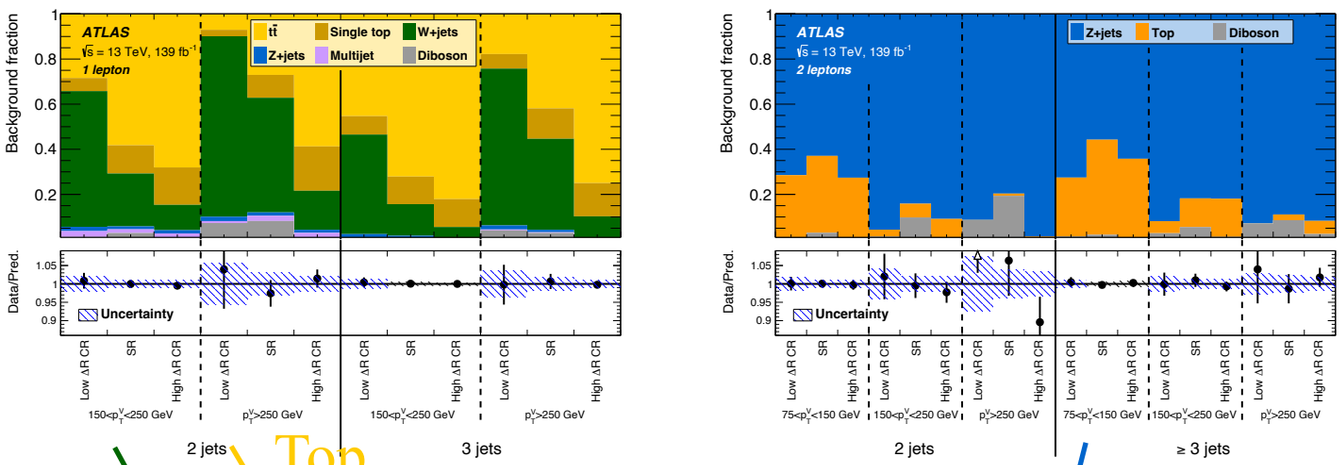

Top

W+jets

Z+jets

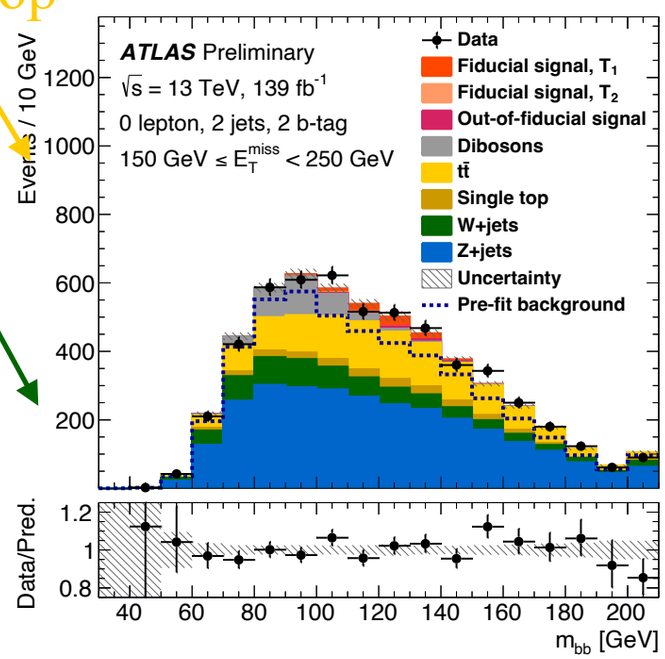

2 fiducial region presented

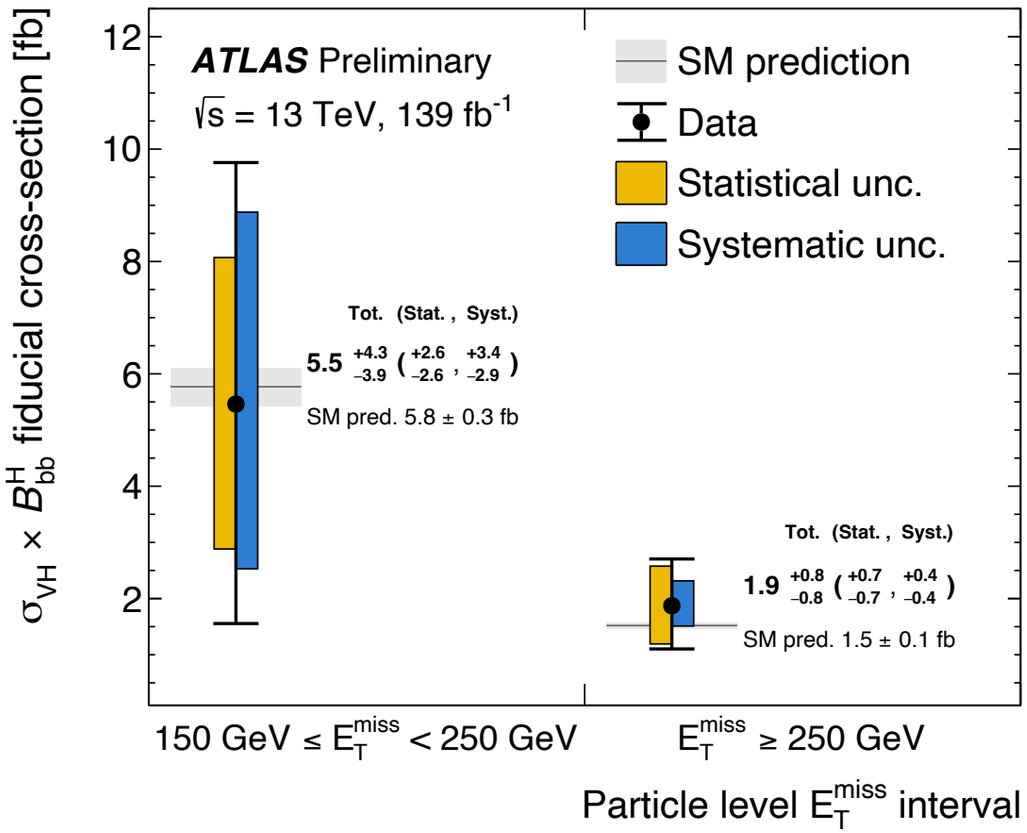

- Good agreement with SM predication
- Useful exercise in view of possible future fiducial measurements in all VH channels

Boosted $H \to b\bar{b}$ channel

Phys. Rev. D 105 (2022) 092003

- Challenging channel but uniquely able to measure the highly boosted regime
  $\Rightarrow$ Reach p_T^H to 1 TeV
- Reconstructed Higgs bosons with large Lorentz boost from single large-radius jets
- Mass of the large-radius jets ~ Higgs boson mass, used as final discriminant
- Main background: QCD Multijet

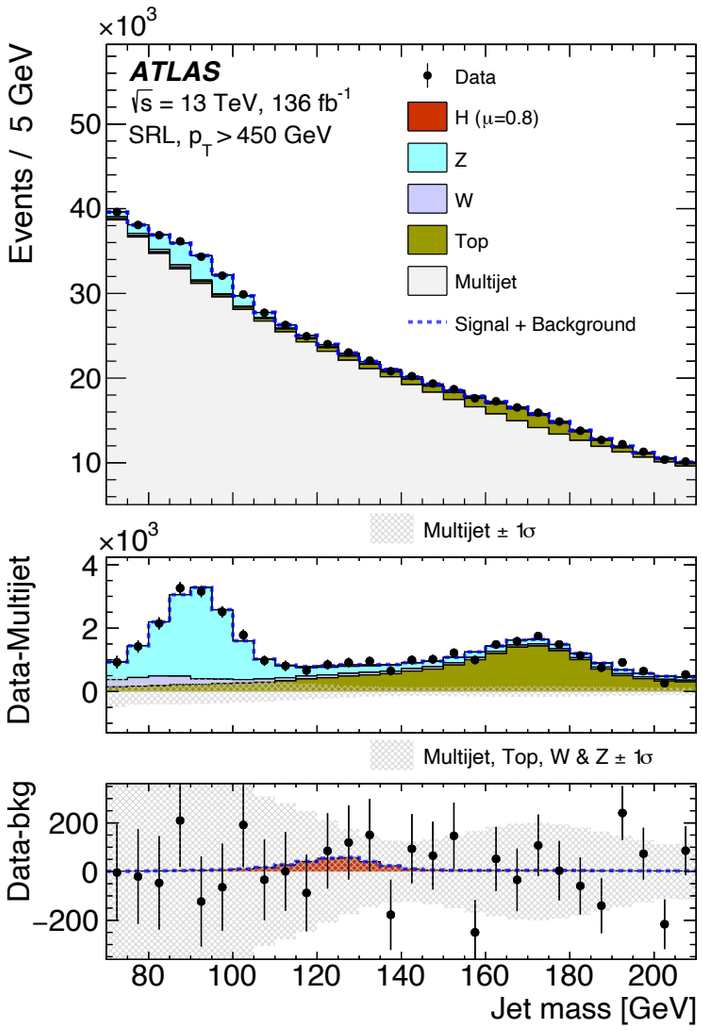

Cross-section limit

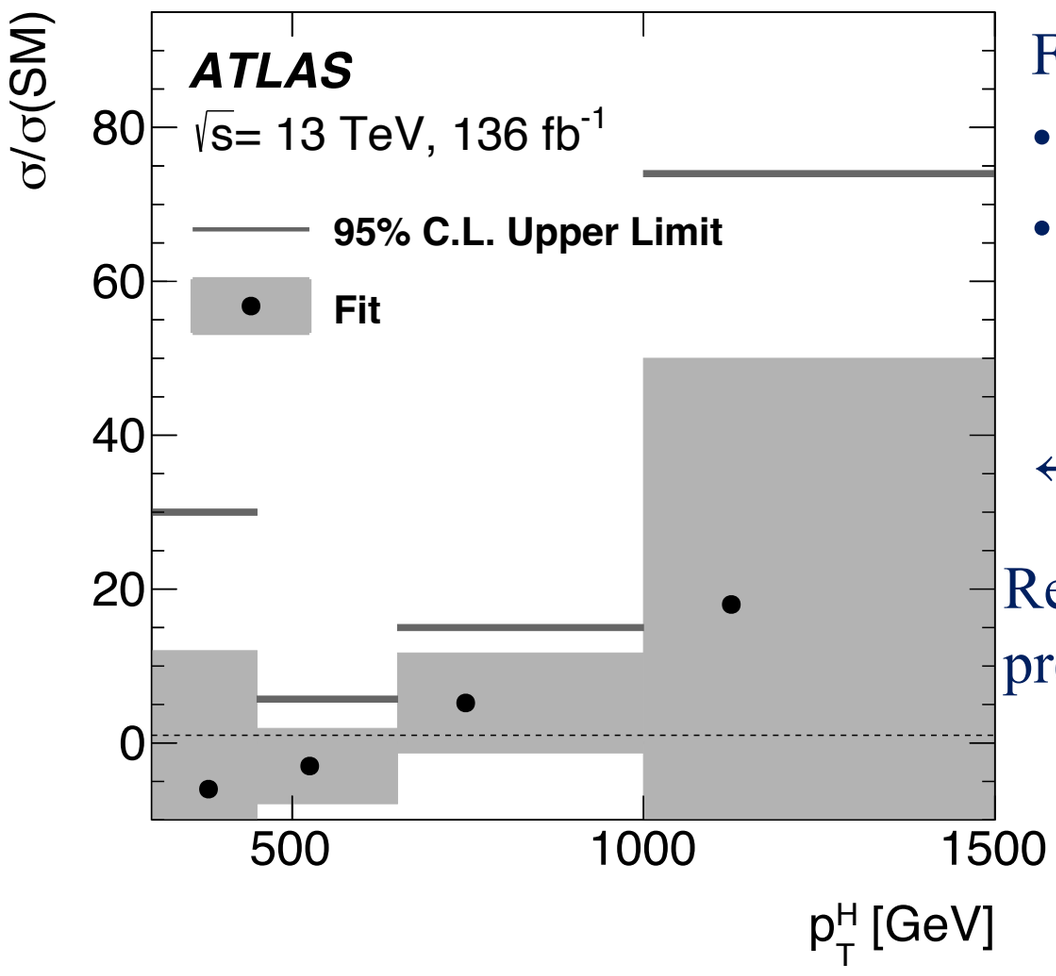

Fiducial region:

- $p_T^H > 450$ GeV, $|y_H| < 2.0$
- $\sigma_{fid} < 115$ fb @ 95% CL
  SM 18.4 fb

← Provide 4 p_T^H volumes

Results are compatible with SM predictions within the uncertainty

ATLAS Run 2 Higgs cross-section results